

Structure Learning with Continuous Optimization: A Sober Look and Beyond

Ignavier Ng¹ Biwei Huang² Kun Zhang^{1,3}

¹Carnegie Mellon University

²University of California San Diego

³Mohamed bin Zayed University of Artificial Intelligence

Abstract

This paper investigates in which cases continuous optimization for directed acyclic graph (DAG) structure learning can and cannot perform well and why this happens, and suggests possible directions to make the search procedure more reliable. [Reisach et al. \(2021\)](#) suggested that the remarkable performance of several continuous structure learning approaches is primarily driven by a high agreement between the order of increasing marginal variances and the topological order, and demonstrated that these approaches do not perform well after data standardization. We analyze this phenomenon for continuous approaches assuming equal and non-equal noise variances, and show that the statement may not hold in either case by providing counterexamples, justifications, and possible alternative explanations. We further demonstrate that nonconvexity may be a main concern especially for the non-equal noise variances formulation, while recent advances in continuous structure learning fail to achieve improvement in this case. Our findings suggest that future works should take into account the non-equal noise variances formulation to handle more general settings and for a more comprehensive empirical evaluation. Lastly, we provide insights into other aspects of the search procedure, including thresholding and sparsity, and show that they play an important role in the final solutions.

1 Introduction

Bayesian networks are a class of probabilistic graphical models that encode probabilistic distributions in a compact way ([Pearl, 1988](#); [Koller and Friedman, 2009](#)). Recovery of their graphical structures from data, represented by directed acyclic graphs (DAGs), has found applications in several fields such as genetics ([Peters et al., 2017](#)) and education ([Gong et al., 2022](#)). This problem is NP-hard in general ([Chickering, 1996](#); [Chickering et al., 2004](#)) owing to the combinatorial space of DAGs.

Classical structure learning approaches fall into two broad categories, i.e., constraint-based methods and score-based methods. Constraint-based methods, such as PC ([Spirtes and Glymour, 1991](#)), employ conditional independence tests to estimate the skeleton and further perform edge orientation up to the Markov equivalence class (MEC) ([Spirtes et al., 2001](#)). Score-based methods typically assign a score to each structure and search for a high-scoring structure in the space of DAGs or equivalence classes ([Koivisto and Sood, 2004](#); [Singh and Moore, 2005](#); [Cussens, 2011](#); [Yuan and Malone, 2013](#)). These methods often adopt greedy search because of the large space of possible structures ([Chickering, 1996](#)), such as GES ([Chickering, 2002](#)) and GDS ([Peters and Bühlmann, 2013](#)).

Recently, [Zheng et al. \(2018\)](#) proposed a smooth characterization of acyclicity and transformed the structure learning problem of discrete nature into a continuous, nonconvex optimization problem, thus enabling the application of gradient-based methods. This formulation has been extended and applied to a wide range of settings, such as nonlinear cases ([Yu et al., 2019](#); [Lachapelle et al., 2020](#); [Zheng et al., 2020](#); [Ng et al., 2022c](#)), interventional data ([Brouillard et al., 2020](#); [Faria et al., 2022](#)), unmeasured confounding ([Bhattacharya et al., 2021](#)), time series ([Pamfil et al., 2020](#)), multi-domain data ([Zeng et al., 2021](#)), federated

learning (Ng et al., 2022a; Gao et al., 2022), domain adaptation (Yang et al., 2021b), and representation learning (Yang et al., 2021a).

Given the growing interest in continuous structure learning, various technical issues of these approaches, both from the theoretical and practical aspects, have gained considerable attention. Specifically, Wei et al. (2020); Ng et al. (2022b) studied the optimality conditions and convergence property of continuous constrained approaches proposed by Zheng et al. (2018). Zhang et al. (2022); Bello et al. (2022) showed that the DAG constraints developed by Zheng et al. (2018); Yu et al. (2019) may encounter gradient vanishing issues in practice and proposed improved variants. Reisach et al. (2021) suggested that the remarkable performance of several continuous structure learning approaches (Zheng et al., 2018; Ng et al., 2020) is primarily driven by a high agreement between the order of increasing marginal variances and the topological order, and demonstrated that these approaches do not perform well after data standardization. Similar phenomenon was also observed by Kaiser and Sipos (2022). These empirical findings regarding data standardization provide insights into the performance of continuous structure learning, and may at first appear surprising. One of our goals is to provide further analysis of this phenomenon.

Contributions. In this work, we investigate in which cases continuous structure learning approaches can and cannot perform well and why this happens, and suggest possible directions to make the search procedure more reliable. Our contributions are:

- We analyze the statements and observations by Reisach et al. (2021) in the linear case with equal (Section 3.1) and non-equal noise variances (Section 3.2), and show that the statements may not hold in either case by providing counterexamples and justifications. We also provide possible alternative explanations for the observation by Reisach et al. (2021) that continuous structure learning approaches do not perform well after data standardization.
- We show that nonconvexity may be a main concern especially for the non-equal noise variances formulation, while recent advances in continuous structure learning, including search strategies, DAG constraints, and nonlinear approaches, fail to achieve improvement in this case (Section 4). Our findings suggest that future works should take into account the non-equal noise variances formulation to handle more general settings and for a more comprehensive empirical evaluation.
- We provide insights into other aspects of the search procedure, including thresholding (Section 5.1) and sparsity penalty (Section 5.2), and show that they play an important role in the final solutions.

2 Background

In this section, we briefly describe several continuous structure learning approaches that this work focuses on, and discuss the notion of varsortability proposed by Reisach et al. (2021).

2.1 Structure Learning with Continuous Optimization

Setup. Let G be a DAG with node set $\{X_1, \dots, X_d\}$. In a Bayesian network, each node X_i of G corresponds to a random variable, and the distribution of the random vector $X = (X_1, \dots, X_d)$, denoted as $P(X)$, is Markov w.r.t. DAG G . In this paper, we consider the linear case in which X follows the linear structural equation model (SEM) $X = B^T X + N$, where $B \in \mathbb{R}^{d \times d}$ is the weighted adjacency matrix associated with DAG G , and $N = (N_1, \dots, N_d)$ is a random noise vector with covariance matrix $\Omega = \text{cov}(N) = \text{diag}(\sigma_1^2, \dots, \sigma_d^2)$. If $\sigma_1^2 = \dots = \sigma_d^2$, we refer to it as the equal noise variances (EV) case, and otherwise as the non-equal noise variances (NV) case. Structure learning aims at estimating the DAG G or its MEC given the data matrix $\mathbf{X} \in \mathbb{R}^{n \times d}$ consisting of n i.i.d. samples from distribution $P(X)$.

NOTEARS. Zheng et al. (2018) proposed to solve the following constrained optimization problem

$$\begin{aligned} \min_{B \in \mathbb{R}^{d \times d}} \ell(B; \mathbf{X}) &:= \frac{1}{2n} \|\mathbf{X} - \mathbf{X}B\|_F^2 \\ \text{subject to } h(B) &= 0, \end{aligned}$$

where $\ell(B; \mathbf{X})$ is the least squares objective and $h(B) := \text{tr}(e^{B \odot B}) - d$ is the DAG constraint term. An ℓ_1 penalty term $\lambda \|B\|_1$ is also incorporated into the objective function, where $\|\cdot\|_1$ is defined element-wise and λ is a hyperparameter. Since the above formulation focuses on the linear case with equal noise variances (Peters and Bühlmann, 2013; Loh and Bühlmann, 2014), we refer to it as NOTEARS-EV throughout this paper.

GOLEM. Instead of using a constrained formulation, Ng et al. (2020) solves an unconstrained optimization problem:

$$\min_{B \in \mathbb{R}^{d \times d}} \mathcal{L}(B; \mathbf{X}) - \log |\det(I - B)| + \lambda_1 \|B\|_1 + \lambda_2 h(B), \quad (1)$$

where $\mathcal{L}(B; \mathbf{X})$ is defined as

$$\mathcal{L}_{\text{EV}}(B; \mathbf{X}) = \frac{d}{2} \log \|\mathbf{X} - \mathbf{X}B\|_F^2 \quad \text{and} \quad \mathcal{L}_{\text{NV}}(B; \mathbf{X}) = \frac{1}{2} \sum_{i=1}^d \log \|\mathbf{X}_{\cdot, i} - \mathbf{X}B_{\cdot, i}\|_2^2$$

in the linear Gaussian case with equal and non-equal noise variances, respectively. Here, λ_1 and λ_2 are hyperparameters. The above two variants are referred to as GOLEM-EV and GOLEM-NV, respectively.

2.2 Varsortability

Recently, Reisach et al. (2021) proposed a measure of agreement between the order of increasing marginal variances and the topological order, which is called *varsortability* and denoted by v . Specifically, it is defined as the proportion of directed paths which start from a variable with strictly lower marginal variance than the variable they end in; see Reisach et al. (2021, Section 3.1) for a complete definition. Clearly, $v = 1$ if the marginal variance of each variable is strictly larger than that of its ancestors in the DAG.

Reisach et al. (2021) provided insights into the performance of several continuous structure learning approaches (Zheng et al., 2018; Ng et al., 2020), and suggested that their remarkable performance is primarily driven by high varsortability. In particular, we list some excerpts from Reisach et al. (2021): “Our experiments demonstrate that varsortability dominates the optimization and helps achieve state-of-the-art performance provided the ground-truth data scale”, and “For this reason we focus on the first optimization steps to explain a) why continuous structure learning algorithms that assume equal noise variance work remarkably well in the presence of high varsortability”. For clarity and ease of further analysis, we attempt to provide a partial formulation of the statements (on which this work focuses), separated into two different cases. We provide a further discussion of how these statements are formulated and possible alternative formulations (e.g., Statements 3 and 4) in Appendix A.

Statement 1 (Equal Noise Variances Formulation). *Continuous structure learning approaches that assume equal noise variances, specifically NOTEARS-EV and GOLEM-EV, perform well in the presence of high varsortability.*

Statement 2 (Non-Equal Noise Variances Formulation). *Continuous structure learning approaches that assume non-equal noise variances, specifically GOLEM-NV, perform well in the presence of high varsortability.*

Reisach et al. (2021) demonstrated that the synthetic data used by Zheng et al. (2018); Ng et al. (2020) to benchmark their proposed methods exhibit high varsortability, e.g., higher than 0.94 on average, and that these approaches do not perform well after data standardization which removes such patterns in the marginal variances. Furthermore, Reisach et al. (2021) provided an analysis based on the first gradient step in the optimization of functions $\ell(B; \mathbf{X})$ and $\mathcal{L}_{\text{EV}}(B; \mathbf{X})$, with the conjecture that the first gradient steps play a dominant role in obtaining the final structure.

3 Varsortability and Data Standardization

In this section, we analyze the statements and observations by Reisch et al. (2021) in the linear case with equal and non-equal noise variances formulations, and show that the statements may not hold in either case. That is, continuous structure learning approaches often do not perform well even in the presence of high varsortability. We also provide possible alternative explanations for the observation by Reisch et al. (2021) that continuous structure learning approaches do not perform well after data standardization.

3.1 With Equal Noise Variances Formulation

Varsortability and continuous structure learning. We first take a closer look at Statement 1. Consider the least squares score used by Zheng et al. (2018); Loh and Bühlmann (2014). For bivariate case, say $X = (X_1, X_2)$ with ground truth $X_1 \rightarrow X_2$, Reisch et al. (2021) showed that inferences based on varsortability and least squares are consistent in the sense that $\nu = 1$, i.e., $\text{Var}(X_1) < \text{Var}(X_2)$ if and only if the least squares score computed with $X_1 \rightarrow X_2$ is smaller than that with $X_2 \rightarrow X_1$; see Reisch et al. (2021, Appendix A) for a proof. Therefore, with high varsortability in the bivariate case, i.e., $\nu = 1$, NOTEARS-EV, loosely speaking, is able to return a correct structure in the sample limit assuming that the global minimizer can be found. Therefore, Statement 1 holds in the bivariate case, at least for NOTEARS-EV.

However, the property in the bivariate case above cannot be extended to general cases with more than two variables; see the following example with three variables.

Example 1. Consider the linear SEM over $X = (X_1, X_2, X_3)$ with the following weighted adjacency matrix and noise covariance matrix:

$$B^* = \begin{bmatrix} 0 & 0.6 & 0.5 \\ 0 & 0 & 2 \\ 0 & 0 & 0 \end{bmatrix}, \quad \Omega^* = \begin{bmatrix} 5 & 0 & 0 \\ 0 & 4 & 0 \\ 0 & 0 & 0.5 \end{bmatrix}.$$

Consider

$$\hat{B} = \begin{bmatrix} 0 & 0 & 0 \\ -\frac{185}{79} & 0 & \frac{131}{58} \\ \frac{100}{79} & 0 & 0 \end{bmatrix}.$$

In the large sample limit, we have

$$\text{Var}(X_1) < \text{Var}(X_2) < \text{Var}(X_3) \quad \text{and} \quad \ell(\hat{B}; \mathbf{X}) < \ell(B^*; \mathbf{X}).$$

That is, even in the presence of high varsortability, i.e., $\nu = 1$, the estimation with least squares score will be the structure indicated by \hat{B} , instead of that by B^* , and thus Statement 1 does not hold.

The proof of the example above is straightforward by calculating the marginal variance of $X_i, i = 1, 2, 3$, say via the diagonal entries of $\Sigma^* := (I - B^*)^{-T} \Omega^* (I - B^*)^{-1}$, and computing $\ell(\hat{B}; \mathbf{X})$ and $\ell(B^*; \mathbf{X})$ via function $\ell(B; \mathbf{X}) = \frac{1}{2} \text{tr}((I - B)^T \Sigma^* (I - B))$. Note that the weighted adjacency matrices B^* and \hat{B} correspond to the triangle structures in Figures 1a and 1b, respectively. In this case, a discrete exhaustive search in the space of DAGs with least squares score returns the wrong structure in Figure 1b, and similarly for NOTEARS-EV assuming the global minimizer can be found. This is also the case for GOLEM-EV because $\mathcal{L}_{\text{EV}}(\hat{B}; \mathbf{X}) < \mathcal{L}_{\text{EV}}(B^*; \mathbf{X})$. To verify it, we conduct 100 simulations using B^* and Ω^* defined in Example 1, and generate 10^6 random samples in each of them. In all simulations, we have $\text{Var}(X_1) < \text{Var}(X_2) < \text{Var}(X_3)$, and observe that NOTEARS-EV and exhaustive search with least squares score return the structure in Figure 1b. Note that GOLEM-EV also does not return the correct structure in all simulations. In the example above, even in the presence of high varsortability, i.e., $\nu = 1$, NOTEARS-EV and GOLEM-EV return a completely inaccurate structure, which indicates that Statement 1 does not hold in general.

One may wonder whether the parameters of B^* and Ω^* in Example 1 have to be exactly “tuned” to obtain such an outcome, which is analogous to the violation of faithfulness assumption (Spirtes et al., 2001) that

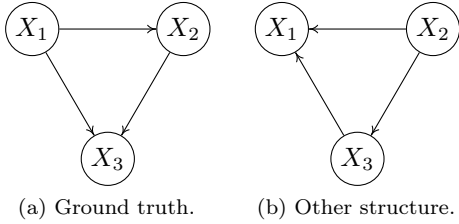


Figure 1: Examples of triangle structures.

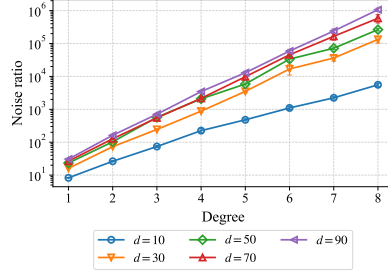


Figure 2: Noise ratio after data standardization

occurs with Lebesgue measure zero. We show that this is not the case, at least for three-variable setting, via the following proposition; specifically, such counterexample exists for a set of distributions with nonzero Lebesgue measure. The proof is given in Appendix B.

Proposition 1. *Consider the distributions induced by linear SEMs over $X = (X_1, X_2, X_3)$. The set of distributions such that varsortability equals one and that the true DAG does not have the lowest least squares score in the large sample limit has a nonzero Lebesgue measure.*

An alternative explanation by noise ratio. Therefore, Statement 1 does not hold in general, and thus may not explain why NOTEARS-EV does not perform well after data standardization. Here, we provide a possible alternative explanation of this phenomenon, i.e., the theoretical guarantee of the least squares score used by NOTEARS-EV does not accommodate the data standardization in general; therefore, such phenomenon may not be surprising. Specifically, Loh and Bühlmann (2014, Theorem 7) showed that, in the large sample limit, minimizing the least squares score in the space of DAGs returns the true structure in the case of linear SEM with equal noise variances. Aragam et al. (2019) established the high dimensional structure consistency with ℓ_1 penalty that includes this case. Moreover, define the noise ratio

$$r = \frac{\max(\sigma_1^2, \dots, \sigma_d^2)}{\min(\sigma_1^2, \dots, \sigma_d^2)},$$

which, intuitively speaking, may be viewed as a way to measure how far the linear SEM is from having equal noise variances. Loh and Bühlmann (2014, Theorem 9) showed that if $r < 1 + \frac{\xi}{d}$, where ξ is defined as the difference between the score of the true DAG and the next best DAG, then, in the large sample limit, minimizing the least squares score in the space of DAGs returns the true structure. This allows a certain degree of misspecification of the noise variances—if the difference ξ is larger, then the least squares score will be more robust to such misspecification. The result in the equal noise variances case (Loh and Bühlmann, 2014, Theorem 7) discussed above can be viewed as a special case in which $r = 1 < 1 + \frac{\xi}{d}$.

Therefore, assuming that the global minimizer can be found, NOTEARS-EV, loosely speaking, is able to return the true DAG in the large sample limit under the assumption specified above, i.e., $r < 1 + \frac{\xi}{d}$. However, after data standardization, this assumption may no longer hold, i.e., the noise ratio becomes

$$r' = \frac{\max(\sigma_1^2 / \text{Var}(X_1), \dots, \sigma_d^2 / \text{Var}(X_d))}{\min(\sigma_1^2 / \text{Var}(X_1), \dots, \sigma_d^2 / \text{Var}(X_d))},$$

and there is no guarantee that $r' < 1 + \frac{\xi'}{d}$. In this case, Theorem 9 of Loh and Bühlmann (2014) does not apply and we are left with no guarantee that NOTEARS-EV or least-squares-based methods can return the true structure. Therefore, they may not perform well after data standardization, and the observation by Reisach et al. (2021) may not be surprising.

In fact, after data standardization, the data may be far from having equal noise variances, i.e., the noise ratio r' may be very large. An example is provided in Figure 2, in which we conduct 1000 random simulations

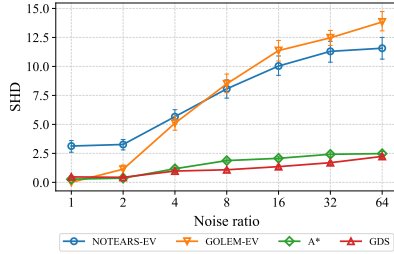


Figure 3: Linear Gaussian-EV formulation without data standardization.

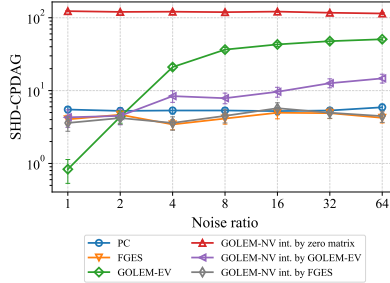


Figure 4: Linear Gaussian-NV formulation without data standardization.

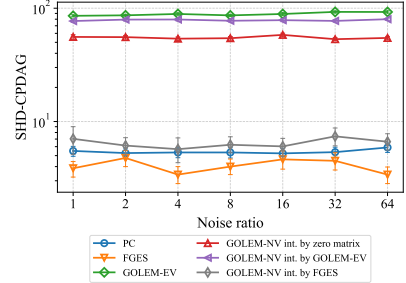


Figure 5: Linear Gaussian-NV formulation with data standardization.

on linear Gaussian-EV model and Erdős–Rényi (Erdős and Rényi, 1959) graphs with varying number of variables and degrees, and further compute the noise ratio in the large sample limit after standardizing the data. One observes that a larger number of variables and degree leads to a higher noise ratio r' ; in this setting considered, the noise ratio appears to increase approximately exponentially in the degree. For example, for 50-node graphs with degree of 4, i.e., the largest number of variables and degrees considered by Reisach et al. (2021), the noise ratio r' is 2079.30 ± 189.6 , which is far from the equal noise variances case.

With such a large noise ratio r' in the scenarios above, the guarantee (Loh and Bühlmann, 2014, Theorem 9) of least squares may not apply after standardization. In other words, least-squares-based search methods, whether it be continuous or discrete ones, are not expected to perform well after standardizing the data.

Empirical studies. To validate the argument above, we compare the performance of different structure learning methods that assume equal noise variances for different noise ratios r . Following previous work (Zheng et al., 2018; Ng et al., 2020), we simulate Erdős–Rényi (Erdős and Rényi, 1959) graphs with kd edges, denoted as ERk , where k represents the average degree. Unless otherwise stated, each edge weight in the true weighted adjacency matrix B is sampled uniformly from $[-2, 0.5] \cup [0.5, 2]$. Here, we consider $ER1$ graphs with number of variables $d \in \{15, 50\}$ and sample size $n \in \{100, 10^6\}$. We use Gaussian noises where the noise variances of two randomly chosen variables are set to 1 and r , respectively, while the variances of the other variables are sampled uniformly from interval $[1, r]$. Here, we consider $r \in \{1, 2, 4, 8, 16, 32, 64\}$. Apart from continuous approaches such as NOTEARS-EV and GOLEM-EV, we also consider discrete approaches, including a greedy approach GDS (Peters and Bühlmann, 2013) and an exact approach A^* (Yuan and Malone, 2013). For both discrete approaches, we use least squares as the score function. Further details about these approaches are provided in Appendix D.1. We report the structural hamming distance (SHD), F1 score, and recall over 30 simulations.

The experiment results for $d = 15$ and $n = 10^6$ are shown in Figure 3, while complete results are available in Figure 14 in Appendix E.1. As the noise ratio increases, the performance of all four methods deteriorates in all cases, especially for continuous approaches like NOTEARS-EV and GOLEM-EV. This demonstrates that, even with a large sample size, these methods that assume equal noise variances are not expected to perform well when the noise ratio r is large. As shown in Figure 2, the noise ratio after data standardization r' is very large, e.g., could be as large as 10^6 , which is much larger than that considered in our experiment here. Thus, it may not be surprising that the structure learning methods considered do not perform well.

3.2 With Non-Equal Noise Variances Formulation

We next turn to the general linear Gaussian case, i.e., the non-equal noise variances formulation. We provide two arguments to explain why Statement 2 may not hold.

Argument 1. *GOLEM-NV often does not perform well in the presence of high varsortability.* We demonstrate that GOLEM-NV with the standard initialization scheme (i.e., zero matrix) does not perform well

Table 1: Empirical results of structure learning methods.

	GOLEM-NV	PC	FGES
SHD of CPDAG	120.3 ± 2.9	5.5 ± 0.5	4.7 ± 0.7
F1 of skeleton	0.50 ± 0.0	0.99 ± 0.0	1.00 ± 0.0
F1 of arrows	0.03 ± 0.0	0.99 ± 0.0	1.00 ± 0.0

in the presence of high varsortability, by comparing its estimated completed partially DAGs (CPDAGs) to standard methods like PC (Spirtes and Glymour, 1991) and FGES (Ramsey et al., 2017). Note that the optimization problem of GOLEM-NV returns a DAG, and therefore an extra step is needed to convert it into a CPDAG. We consider linear Gaussian models with 50 variables and ER1 graphs, where the noise ratio r is 2. The sample size is set to $n = 10^6$ to ensure that it is sufficiently large. Here, the varsortability is 0.97 ± 0.003 , which is consistent with the high varsortability reported by Reisach et al. (2021, Section 3.3).

The results in Table 1 show that PC and FGES can nearly recover the true CPDAG with a high F1 score, while GOLEM-NV has a low F1 score and high SHD. Note that the performance of GOLEM-NV is worse than an empty graph whose SHD is 50. Therefore, GOLEM-NV does not perform well in the presence of high varsortability, and it seems that high varsortability does not help GOLEM-NV achieve a remarkable performance. The question is then why Ng et al. (2020) observed a remarkable performance for GOLEM-NV on synthetic data as noticed by Reisach et al. (2021), which we address next.

Argument 2. *The quality of the final solution estimated by GOLEM-NV depends largely on the initial solution possibly owing to nonconvexity.* Ng et al. (2020, Section 4.1) adopted an initialization scheme for GOLEM-NV which uses the solution returned by GOLEM-EV as the initial solution, because the authors noticed that the optimization procedure of GOLEM-NV is prone to local solutions. Here, we conduct experiments with different initialization schemes and find that they play an important role in the quality of the final solutions, possibly because of the nonconvex optimization formulation.

Empirical studies. We consider 50-variable linear Gaussian model with ER1 graphs and noise ratios $r \in \{1, 2, 4, 8, 16, 32, 64\}$. We use a large sample size 10^6 to reduce the errors caused by finite samples and to focus on the aspect of nonconvex optimization. We experiment with different initialization schemes, including GOLEM-NV initialized by zero matrix, by solution of GOLEM-EV, and by solution of FGES¹.

The experiment results of SHD before and after standardization are available in Figures 4 and 5, where the other metrics are available in Figure 15 in Appendix E.2. Consistent with the empirical study in Table 1, GOLEM-NV initialized by zero matrix does not perform well across all settings. Furthermore, before data standardization, the performance of GOLEM-EV and GOLEM-NV initialized by GOLEM-EV exhibit similar trend, both of which degrade as the noise ratio increases, and their gap with PC and FGES is also enlarged. A possible reason is that GOLEM-NV may be susceptible to suboptimal local solutions owing to nonconvexity, and thus its performance largely depends on the quality of solution of GOLEM-EV. However, as the noise ratio increases, the quality of solution returned by GOLEM-EV deteriorates, as discussed in Section 3.1; therefore, in this case GOLEM-NV no longer has an initial solution of decent quality. Similar explanation may also apply to its results after data standardization, i.e., GOLEM-NV initialized by GOLEM-EV has a poor performance after data standardization (also observed by Reisach et al. (2021)) because GOLEM-EV does not perform well owing to the large noise ratio r' , as discussed in Section 3.1. By contrast, GOLEM-NV initialized by the solution of FGES performs well in all cases, where the results are close to FGES and PC. This is because FGES returns a solution with high quality across different noise ratio r , which serves as a good initial starting point for optimization of GOLEM-NV.

It is worth noting that the optimization problem of GOLEM-NV in Eq. (1) involves only the matrix B because it profiles out the parameter Ω that corresponds to the noise variances; see Ng et al. (2020,

¹Since FGES returns a CPDAG, we generate a DAG consistent with it following the procedure developed by Dor and Tarsi (1992), and compute the least squares coefficients for this specific DAG.

Appendix C.1) for more details about the derivation. We further consider the form of likelihood function without profiling out such parameter and observe that it also leads to a poor performance when initialized with zero matrix, similar to the original version of GOLEM-NV. Further details and experiment results are provided in Appendix C.1.

Instead of high varsortability, the observations above suggest that the performance of GOLEM-NV largely depends on the initial solution. A possible reason is that the optimization problem of GOLEM-NV may be highly nonconvex and contain many suboptimal local solutions, because (1) a large sample size $n = 10^6$ is used which leads to small finite-sample errors, and (2) GOLEM-NV has been shown to be consistent under mild conditions, assuming that the global minimizer can be found and ℓ_0 penalty is used (note that Ng et al. (2020) did not provide guarantee for ℓ_1 penalty).² This is in stark contrast with the observation by Zheng et al. (2018, Section 5.3) for the equal noise variances formulation, i.e., the solutions of NOTEARS-EV are in practice close to the global minimizer. We provide further analysis on the nonconvexity of GOLEM-NV in Appendix C.2. Moreover, the above empirical studies may explain the remarkable performance of GOLEM-NV in the synthetic data experiments in Ng et al. (2020), as noticed by Reisach et al. (2021), which simulate linear Gaussian model with a relatively small noise ratio $r \leq 4$. In this case, GOLEM-EV achieves a decent performance, and using its solution to initialize GOLEM-NV leads to a remarkable performance.

4 Nonconvexity of Non-Equal Noise Variances Formulation

The empirical studies in Section 3.2 suggest that continuous structure learning approach that assumes non-equal noise variances, specifically GOLEM-NV, is prone to suboptimal local solutions, possibly owing to nonconvexity. On the other hand, many existing works (Zheng et al., 2018; Yu et al., 2021; Charpentier et al., 2022; Bello et al., 2022) considered the equal noise variances formulation (by adopting least squares objective) and observed remarkable performance. This suggests that the nonconvexity issue might be less severe for the equal noise variances formulation. In this section, we demonstrate that these recent advances for the equal noise variances formulation fail to achieve improvement for the non-equal noise variances formulation, thus suggesting that nonconvexity may be a key concern for the latter formulation. Specifically, we consider recently developed search strategies and DAG constraints in Sections 4.1 and 4.2, respectively, and other cases in Section 4.3, namely linear non-Gaussian and nonlinear cases.

4.1 Search Strategies

Methods. We consider different search strategies, namely NOTEARS (Zheng et al., 2018), DAGMA (Bello et al., 2022), GOLEM (Ng et al., 2020), NOCURL (Yu et al., 2021), and DPDAG (Charpentier et al., 2022), to investigate if they perform well for the non-equal noise variances formulation. These methods represent different strategies to traverse the search space for estimating a DAG with continuous optimization; a summary of them is provided in Appendix D.2. For NOTEARS, DAGMA, NOCURL, and DPDAG, we replace their least squares objective $\ell(B; \mathbf{X})$ with $\mathcal{L}_{\text{NV}}(B; \mathbf{X})$, which correspond to the likelihood of linear Gaussian DAGs assuming non-equal noise variances; see Ng et al. (2020, Appendix C.1) for a detailed derivation, where the term $-\log |\det(I - B)|$ is omitted because a hard DAG constraint is used for these methods. We denote the resulting methods by NOTEARS-NV, DAGMA-NV, NOCURL-NV, and DPDAG-NV, respectively. We consider linear Gaussian model with 50-node ER1 graphs and noise ratio r of 16. We consider $n \in \{10^2, 10^3, 10^4, 10^5, 10^6\}$.

Experiment results. The experiment results of SHD computed over CPDAGs are available in Figure 6, where the other metrics are available in Figure 16 in Appendix E.3. It is observed that none of the continuous structure learning approaches perform well, compared to PC and FGES. For PC and FGES, as the sample size increases, PC and FGES improve with a larger sample size and eventually reach SHDs of 7.9 ± 0.6 and 8.3 ± 0.6 , respectively. By contrast, the quality of solution estimated by continuous structure learning

²With global minimizer and ℓ_0 penalty, the theoretical guarantee of GOLEM-NV (Ng et al., 2020, Theorem 2) holds in the large sample limit under the corresponding conditions, regardless of the initial solution and whether the data is standardized.

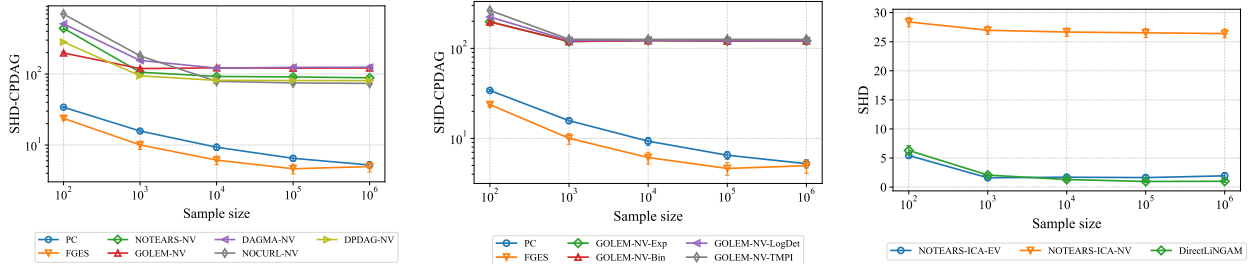


Figure 6: Different search strategies. Figure 7: Different DAG constraints. Figure 8: Linear non-Gaussian case.

approaches does not improve much with a larger sample size and reaches a performance plateau after $n = 10^3$. Specifically, the SHD of these continuous approaches is larger than 70 even when the sample size is $n = 10^6$. Note that an empty graph has an SHD of 50. A possible reason is that the optimization problem of these continuous approaches may be highly nonconvex and contain many suboptimal local solutions, thus leading to estimated CPDAGs that are far from the true ones.

4.2 DAG Constraints

Methods. We consider the DAG constraints commonly adopted by continuous structure learning approaches based on matrix exponential (Zheng et al., 2018) and binomial (Yu et al., 2019), as well as more recent DAG constraints based on log-determinant (Bello et al., 2022) and truncated geometric series (Zhang et al., 2022) that have been demonstrated to be less sensitive to the gradient vanishing issue encountered by the former two constraints. We apply these four constraints to GOLEM-NV, denoted as GOLEM-NV-Exp, GOLEM-NV-Bin, GOLEM-NV-LogDet, and GOLEM-NV-TMPI, respectively, and similarly for NOTEARS-NV.

Experiment results. Here we use the same setup of simulated data as that of Section 4.1. The SHDs of GOLEM-NV are depicted in Figure 7, while complete results including those for NOTEARS-NV are available in Figure 17 in Appendix E.4. Similar to the observation in Section 4.1, one observes that GOLEM-NV and NOTEARS-NV equipped with these DAG constraints quickly reach a performance plateau and do not improve much with increasing sample sizes. Specifically, the SHDs of GOLEM-NV and NOTEARS-NV with these DAG constraints are larger than 120 and 80, respectively. Note that Bello et al. (2022); Zhang et al. (2022) observed that their proposed DAG constraints lead to a huge improvement over those existing ones (Zheng et al., 2018; Yu et al., 2019) for the equal noise variances formulation. Clearly, this experiment demonstrates that such an improvement cannot be translated into the non-equal noise variances formulation, at least in the settings considered here. Furthermore, this suggests that the optimization problem of the non-equal noise variances formulation might be more challenging than the equal noise variances formulation as the former may contain more suboptimal local solutions.

4.3 Other Cases

We now investigate whether the observations in previous linear Gaussian experiments generalize to other cases, namely linear non-Gaussian (Shimizu et al., 2006) and nonlinear (Hoyer et al., 2009) cases.

Linear non-Gaussian case. Zheng (2020) developed an extension of NOTEARS to handle linear non-Gaussian case, called NOTEARS-ICA. It is worth noting that Zheng (2020, Section 4.3.2) provided a general formulation in the non-equal noise variances case; as the same time, their experiments, as discussed by Zheng (2020, Section 4.5), seem to adopt the equal noise variances formulation. Here, we consider both equal and non-equal noise variances formulation for NOTEARS-ICA, denoted as NOTEARS-ICA-EV and NOTEARS-ICA-NV, respectively. We simulate 15-node ER1 graphs and linear SEM with standard Laplace

noise. The SHDs are reported in Figure 8, while complete results are shown in Figure 18 in Appendix E.5. We observe that NOTEARS-ICA-EV performs similarly to DirectLiNGAM, both of which improve with more samples; specifically, their SHDs are very close to zero when the sample size is large. However, the performance of NOTEARS-ICA-NV does not improve much even when the sample size is large. For example, when $n = 10^6$, NOTEARS-ICA-EV and DirectLiNGAM have SHDs of 1.93 ± 0.59 and 0.97 ± 0.2 , respectively, while NOTEARS-ICA-NV has SHD of 26.40 ± 0.80 . Note that an empty graph leads to an SHD of 15. This suggests that the optimization problem of NOTEARS-ICA-NV may be more challenging than that of NOTEARS-ICA-EV and contain more suboptimal local solutions.

Nonlinear case. There are several nonlinear extensions of NOTEARS, some of which rely on different pre/post-processing steps like pruning (Lachapelle et al., 2020; Ng et al., 2022c), making it difficult to investigate the performance of continuous optimization procedure. We consider NOTEARS-MLP (Zheng et al., 2020) that does not rely on such pre/post-processing steps, and extend it to the non-equal noise variances formulation by replacing its least squares objective with $\mathcal{L}_{\text{NV}}(B, \mathbf{X})$, in which the residuals are computed with multilayer perceptron (MLP) instead of linear regression. We consider the data generating procedure used by Zheng et al. (2020) with MLPs and standard Gaussian noise. The experiment results are available in Figure 19 in Appendix E.5. Similar to the observation in the linear non-Gaussian case, NOTEARS-MLP-EV achieves a much lower SHD when the sample size is large, while NOTEARS-MLP-NV does not improve much and its SHD remains at 10.1 ± 3.1 even when the sample size is as large as 10^5 .

5 Thresholding and Sparsity Penalty

Apart from the possible nonconvexity issue discussed in Section 4, we show that the performance of continuous approaches is sensitive to other aspects of the search procedure, i.e., thresholding and sparsity.

These technical issues should be made transparent, as they play an important role in the final solutions.

In concurrent work, Xu et al. (2022) also studied the aspects of thresholding and sparsity in NOTEARS-EV. Here, our analysis of thresholding includes GOLEM-EV and discrete approaches such as A* and GDS, as well as both small ($n = 100$) and large ($n = 10^6$) sample sizes; therefore, the analysis and observations are different. For sparsity, Xu et al. (2022) adopted the adaptive ℓ_1 penalty (Zou, 2006) for NOTEARS-EV, while we consider the smoothly clipped absolute deviation (SCAD) penalty (Fan and Li, 2001) and minimax concave penalty (MCP) (Zhang, 2010) for NOTEARS-EV and GOLEM-EV.

5.1 Thresholding

We investigate the impact of threshold specification on continuous structure learning approaches, and show that it plays an important role for the final solutions. Existing continuous approaches (Zheng et al., 2018; Ng et al., 2020; Yu et al., 2021; Bello et al., 2022) typically use edge weights sampled uniformly from $[-2, -0.5] \cup [0.5, 2]$ for the true weighted adjacency matrix and apply a threshold of 0.3 to identify the final structure. Here, we consider 15-node ER1 graphs with different ranges of edge weights $[-2\alpha, -0.5\alpha] \cup [0.5\alpha, 2\alpha]$ where $\alpha \in \{0.25, 0.5, 0.75, 1, 1.25\}$, and sample sizes $n \in \{100, 10^6\}$. Apart from continuous approaches like NOTEARS-EV and GOLEM-EV, we also report results for discrete approaches A* and GDS. The thresholds considered are 0.05, 0.1, 0.2, 0.3, 0.4, 0.5, 0.6. Note that A* and GDS return a DAG, and thus we apply thresholding on its least squares coefficients. The SHDs are provided in Figure 9, while complete results for F1 score and recall are given in Figure 20 in Appendix E.6. The observations are described below.

Observation 1. *When $n = 100$, using a relatively large threshold (e.g., 0.3) is beneficial for all methods considered.* When the sample size is small, the estimated DAGs by both continuous and discrete approaches may contain many false discoveries owing to finite-sample errors, and using a relatively large threshold helps remove some of them. This appears to increase the precision at the cost of decreasing the recall.

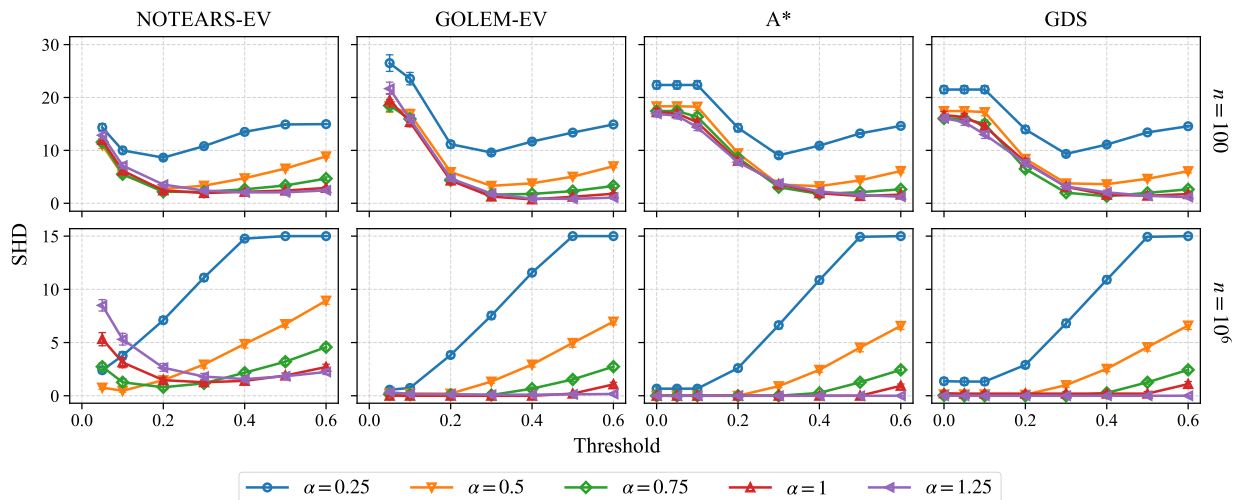


Figure 9: SHDs of different thresholds under different weight scales. The number of variables is 15. Error bars represent the standard errors computed over 30 random repetitions.

Observation 2. When $n = 10^6$, using a relatively large threshold (e.g., 0.3) is harmful in many cases. In this case, using a threshold of 0.3 increases the SHDs of all methods for $\alpha = 0.25, 0.5$, since the recall is decreased. A possible reason is that the threshold applied is larger than many edge weights in the true weighted adjacency matrix. Therefore, the fixed threshold of 0.3 used in existing works may be undesirable in many cases, as it may wrongly remove many edges and lead to a low recall. To avoid such a case, we adopt a relatively small threshold (e.g., 0.1) in the other experiments.

Observation 3. When $\alpha = 1$, the optimal threshold for NOTEARS-EV is 0.3 for $n = 100, 10^6$. Specifically, its SHDs are 1.93 ± 0.36 and 1.27 ± 0.24 for $n = 100, 10^6$, respectively. Moreover, one observes that NOTEARS-EV has different optimal thresholding values across all settings. Since $\alpha = 1$ corresponds to the data generating procedure used by Zheng et al. (2018) and several follow-up works, this indicates that their comparison with existing baselines, particularly discrete approaches, may not be completely fair as it may implicitly assume prior knowledge about the range of the edge weights in the data generating procedure.

Observation 4. When $n = 10^6$, NOTEARS-EV requires a relatively large threshold (e.g., 0.3) to perform well for $\alpha = 0.75, 1, 1.25$, while a small threshold (i.e., 0.05) is sufficient for GOLEM-EV for all α considered. Specifically, with a threshold of 0.05, GOLEM-EV achieves SHDs of $0.57 \pm 0.18, 0.20 \pm 0.10, 0.13 \pm 0.10, 0 \pm 0, 0.33 \pm 0.18$ for $\alpha = 0.25, 0.5, 0.75, 1, 1.25$, respectively, indicating that the estimated DAGs by GOLEM-EV are very close to ground truths. Since the sample size $n = 10^6$ used here is large and leads to considerably small finite-sample errors, this appears to suggest that the nonconvex landscape of GOLEM-EV may contain fewer suboptimal local solutions in this setting; thus, when initialized with a zero matrix, gradient-based optimization procedure reaches a solution that is close to the ground truth. By contrast, this is not the case of NOTEARS-EV, which, with a threshold of 0.05, achieves SHDs of $14.33 \pm 0.70, 11.00 \pm 0.61, 11.53 \pm 0.72, 11.97 \pm 0.68, 12.87 \pm 0.69$ for $\alpha = 0.25, 0.5, 0.75, 1, 1.25$, respectively. For these values of α , a threshold of 0.3 leads to better performance (roughly SHD of 2) for NOTEARS-EV. This indicates that it is more likely for NOTEARS-EV to return suboptimal local solutions as compared to GOLEM-EV, at least in this setting considered where the sample size is large. This observation also suggests that, in addition to reducing false discoveries resulting from finite-sample errors, *thresholding may help reduce false discoveries caused by nonconvexity*, especially for NOTEARS-EV.

It is clear from Observations 1-4 that different approaches have different optimal thresholds in different settings. Therefore, a possible direction is to develop a general procedure (e.g., adaptive thresholding) that

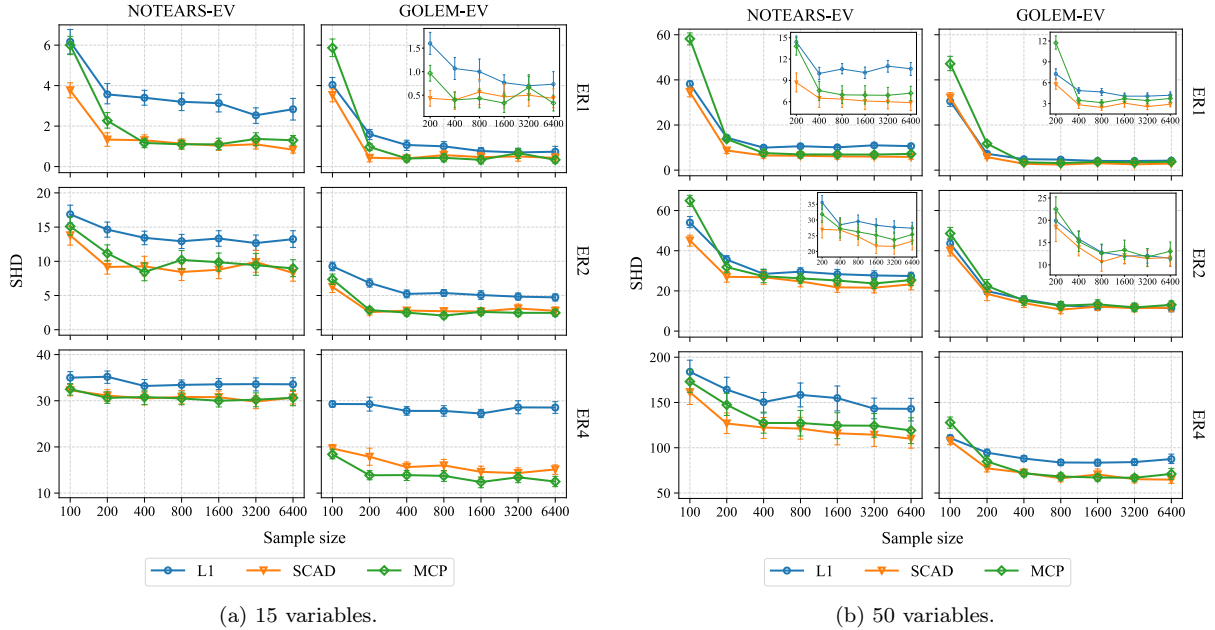


Figure 10: SHDs of different sparsity penalties under different sample sizes. Error bars represent the standard errors computed over 30 random repetitions.

can be reliably applied in different settings to identify edges from the solutions of continuous structure learning approaches. As discussed above, this may also help reduce false discoveries resulting from both finite-sample errors and nonconvexity (see Observation 4).

5.2 Sparsity Penalty

Apart from nonconvexity, another key factor that differentiates continuous structure learning approaches from exact discrete search approaches (e.g., A^* (Yuan and Malone, 2013), dynamic programming (Singh and Moore, 2005)) is that the latter use ℓ_0 penalty, while the former adopt ℓ_1 penalty, which is known to be biased and negatively affect the performance (Fan and Li, 2001; Breheny and Huang, 2011). The reason is that it penalizes all coefficients with the same intensity, including those with small values. Thus, we consider alternative forms of sparsity penalty that help overcome such an issue, namely the smoothly clipped absolute deviation (SCAD) penalty (Fan and Li, 2001) and minimax concave penalty (MCP) (Zhang, 2010), where large coefficients are penalized less than small ones. Moreover, SCAD penalty and MCP do not require the incoherence condition for support recovery (Loh and Wainwright, 2017) that is needed by ℓ_1 penalty in several statistical problems (Wainwright, 2009; Ravikumar et al., 2011), which might be a rather restrictive assumption in practice. This is also the case for structure learning—Aragam et al. (2019) established high dimensional structure consistency of the least squares estimator in the space of acyclic weighted adjacency matrices (which corresponds to the formulation of NOTEARS), for which the incoherence condition is not needed when MCP is used.

We compare the performance of NOTEARS-EV and GOLEM-EV under specification of the sparsity penalties discussed above. We consider ER1, ER2, and ER4 graphs with graph size $d \in \{15, 50\}$ and sample size $n \in \{100, 200, 400, 800, 1600, 3200, 6400\}$. The SHDs are reported in Figure 10, and complete results are provided in Figure 21 in Appendix E.7. In most settings, we observe that SCAD penalty and MCP achieve significant improvement over ℓ_1 penalty for both NOTEARS-EV and GOLEM-EV, especially when the degree is large. For 15-node graphs, SCAD penalty and MCP lead to similar performance, while SCAD penalty slightly outperforms MCP on 50-node graphs.

One may wonder how different specifications of the sparsity penalty considered above compare to ℓ_0 penalty. Since SCAD penalty and MCP perform similarly, we compare GOLEM-EV and NOTEARS-EV equipped with the SCAD penalty to discrete approaches, i.e., A^* and GDS, that rely on ℓ_0 penalty. We consider 15-node ER2 graphs with varying sample sizes, and report the SHDs in Figure 11. Comparing NOTEARS-EV, A^* , and GDS that all use the least squares objective, one observes that A^* , not surprisingly, has the lowest SHDs, while GDS is on par with it. On the other hand, NOTEARS-EV has a much higher SHD than that of GDS. That is, NOTEARS-EV, even with the SCAD penalty, performs much worse than a greedy search method such as GDS, not to mention exact search method like A^* . Such a performance gap conveys a cautionary message that continuous structure learning approaches may be inevitably susceptible to the nonconvexity issue that might be severe in practice. This is in contrast with the observation by [Zheng et al. \(2018, Section 5.3\)](#) that the estimated solutions by NOTEARS-EV are very close to the global minimizers despite its nonconvexity. A possible reason is that we apply a relatively small threshold 0.1, and as discussed in Section 5.1, NOTEARS-EV may require a larger threshold, e.g., 0.3, to achieve a decent performance, possibly owing to nonconvexity.

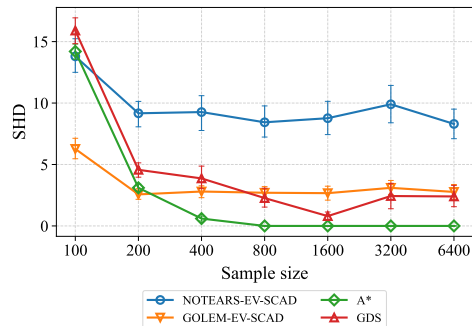


Figure 11: SCAD and ℓ_0 penalties.

6 Conclusion and Discussion

We investigate in which cases continuous structure learning approaches can and cannot perform well and why this happens. We focus on several specifications of the data and search procedure, including varsortability, data standardization, nonconvexity, thresholding, and sparsity. Despite the simplicity of continuous structure learning approaches, we demonstrate that they may suffer from various technical issues discussed below. Our goal here is not to resolve all these issues, but rather to analyze and make them transparent, as well as suggesting possible directions. We hope that our studies could stimulate future works on developing more reliable continuous structure learning approaches, e.g., to overcome the nonconvexity and thresholding issues. Detailed discussions are provided below.

Varsortability and data standardization. We show that the statements by [Reisach et al. \(2021\)](#) may not hold in the linear case with equal and non-equal noise variances, and provide possible alternative explanations for the observation by [Reisach et al. \(2021\)](#) that continuous structure learning approaches do not perform well after data standardization. For the equal noise variances formulation, we provide counterexamples to the statement, and demonstrate that the performance of continuous approaches assuming equal noise variances degrade as the noise ratio increases, which may explain why they do not perform well after data standardization. For the non-equal noise variances formulation, we show that nonconvexity may be the reason why continuous approaches do not perform well both before and after data standardization.

Nonconvexity. Many existing works in continuous structure learning considered only the equal noise variances formulation by adopting least squares objective and observed remarkable performance. We demonstrate that these recent advances for the equal noise variances formulation fail to achieve improvement for the non-equal noise variances formulation. This suggests that nonconvexity may be a main concern especially for the latter formulation. Our findings suggest that future works should take into account the non-equal noise variances formulation to handle more general settings and for a more comprehensive empirical evaluation, and develop reliable approaches that mitigates the nonconvexity issue.

Thresholding. Our empirical studies demonstrate that the choice of threshold plays an important role in the final solutions, and that optimal thresholds may differ across settings. Specifically, (1) using a relatively

large threshold of 0.3 as in existing works may be harmful and remove many true edges, especially when the edge weights in the true weighted adjacency matrix are small. (2) Thresholding may be beneficial in certain cases as it not only helps reduce false discoveries resulting from finite-sample errors, but may also help reduce those caused by nonconvexity, especially for NOTEARS. Therefore, the choice of threshold should be treated with care. A possible future direction is to develop a general procedure (e.g., adaptive thresholding) that can be reliably applied in different settings to identify edges from the solutions of continuous structure learning approaches, while also reducing false discoveries arising from nonconvexity.

Sparsity penalty. We demonstrate that the specification of sparsity penalty plays an important role for continuous structure learning approaches like GOLEM-EV and NOTEARS-EV. Specifically, ℓ_1 penalty may not perform well possibly due to its bias, while other penalties like SCAD and MCP could help remedy it.

References

- B. Aragam, A. Amini, and Q. Zhou. Globally optimal score-based learning of directed acyclic graphs in high-dimensions. In *Advances in Neural Information Processing Systems*, volume 32, 2019.
- J. Bang-Jensen and G. Gutin. *Digraphs. Theory, Algorithms and Applications*. Springer Monographs in Mathematics, 2009.
- K. Bello, B. Aragam, and P. Ravikumar. DAGMA: Learning DAGs via M-matrices and a log-determinant acyclicity characterization. In *Advances in Neural Information Processing Systems*, 2022.
- D. P. Bertsekas. *Constrained Optimization and Lagrange Multiplier Methods*. Academic Press, 1982.
- D. P. Bertsekas. *Nonlinear Programming*. Athena Scientific, 2nd edition, 1999.
- R. Bhattacharya, T. Nagarajan, D. Malinsky, and I. Shpitser. Differentiable causal discovery under unmeasured confounding. In *International Conference on Artificial Intelligence and Statistics*, 2021.
- P. Breheny and J. Huang. Coordinate descent algorithms for nonconvex penalized regression, with applications to biological feature selection. *The Annals of Applied Statistics*, 5(1):232–253, 2011.
- P. Brouillard, S. Lachapelle, A. Lacoste, S. Lacoste-Julien, and A. Drouin. Differentiable causal discovery from interventional data. In *Advances in Neural Information Processing Systems*, 2020.
- R. H. Byrd, P. Lu, J. Nocedal, and C. Zhu. A limited memory algorithm for bound constrained optimization. *SIAM Journal on Scientific Computing*, 16(5):1190–1208, 1995.
- B. Charpentier, S. Kibler, and S. Günnemann. Differentiable DAG sampling. In *International Conference on Learning Representations*, 2022.
- D. M. Chickering. Learning Bayesian networks is NP-complete. In *Learning from Data: Artificial Intelligence and Statistics V*. Springer, 1996.
- D. M. Chickering. Optimal structure identification with greedy search. *Journal of Machine Learning Research*, 3(Nov):507–554, 2002.
- D. M. Chickering, D. Heckerman, and C. Meek. Large-sample learning of Bayesian networks is NP-hard. *Journal of Machine Learning Research*, 5, 2004.
- J. Cussens. Bayesian network learning with cutting planes. In *Conference on Uncertainty in Artificial Intelligence*, 2011.
- D. Dor and M. Tarsi. A simple algorithm to construct a consistent extension of a partially oriented graph. *Technical Report R-185, Cognitive Systems Laboratory, UCLA*, 1992.

- P. Erdős and A. Rényi. On random graphs I. *Publicationes Mathematicae*, 6:290–297, 1959.
- J. Fan and R. Li. Variable selection via nonconcave penalized likelihood and its oracle properties. *Journal of the American statistical Association*, 96(456):1348–1360, 2001.
- G. R. A. Faria, A. Martins, and M. A. T. Figueiredo. Differentiable causal discovery under latent interventions. In *Conference on Causal Learning and Reasoning*, 2022.
- E. Gao, J. Chen, L. Shen, T. Liu, M. Gong, and H. Bondell. FedDAG: Federated DAG structure learning. *Transactions on Machine Learning Research*, 2022.
- W. Gong, D. Smith, Z. Wang, C. Barton, S. Woodhead, N. Pawlowski, J. Jennings, and C. Zhang. NeurIPS competition instructions and guide: Causal insights for learning paths in education. *arXiv preprint arXiv:2208.12610*, 2022.
- P. Hoyer, D. Janzing, J. M. Mooij, J. Peters, and B. Schölkopf. Nonlinear causal discovery with additive noise models. In *Advances in Neural Information Processing Systems*, 2009.
- X. Jiang, L.-H. Lim, Y. Yao, and Y. Ye. Statistical ranking and combinatorial Hodge theory. *Mathematical Programming*, 127, 11 2011.
- M. Kaiser and M. Sipos. Unsuitability of NOTEARS for causal graph discovery when dealing with dimensional quantities. *Neural Processing Letters*, 54:1–9, 06 2022.
- D. Kingma and J. Ba. Adam: A method for stochastic optimization. In *International Conference on Learning Representations*, 2014.
- M. Koivisto and K. Sood. Exact Bayesian structure discovery in Bayesian networks. *Journal of Machine Learning Research*, 5(Dec):549–573, 2004.
- D. Koller and N. Friedman. *Probabilistic Graphical Models: Principles and Techniques*. MIT Press, Cambridge, MA, 2009.
- W. Kool, H. Van Hoof, and M. Welling. Stochastic beams and where to find them: The Gumbel-top-k trick for sampling sequences without replacement. In *International Conference on Machine Learning*, 2019.
- S. Lachapelle, P. Brouillard, T. Deleu, and S. Lacoste-Julien. Gradient-based neural DAG learning. In *International Conference on Learning Representations*, 2020.
- P.-L. Loh and P. Bühlmann. High-dimensional learning of linear causal networks via inverse covariance estimation. *Journal of Machine Learning Research*, 15(88):3065–3105, 2014.
- P.-L. Loh and M. J. Wainwright. Support recovery without incoherence: A case for nonconvex regularization. *The Annals of Statistics*, 45(6):2455–2482, 2017.
- G. Mena, D. Belanger, S. Linderman, and J. Snoek. Learning latent permutations with Gumbel-Sinkhorn networks. In *International Conference on Learning Representations*, 2018.
- I. Ng, A. Ghassami, and K. Zhang. On the role of sparsity and DAG constraints for learning linear DAGs. In *Advances in Neural Information Processing Systems*, 2020.
- I. Ng, , and K. Zhang. Towards federated Bayesian network structure learning with continuous optimization. In *International Conference on Artificial Intelligence and Statistics*, 2022a.
- I. Ng, S. Lachapelle, N. R. Ke, S. Lacoste-Julien, and K. Zhang. On the convergence of continuous constrained optimization for structure learning. In *International Conference on Artificial Intelligence and Statistics*, 2022b.

- I. Ng, S. Zhu, Z. Fang, H. Li, Z. Chen, and J. Wang. Masked gradient-based causal structure learning. In *SIAM International Conference on Data Mining*, 2022c.
- J. Nocedal and S. J. Wright. *Numerical optimization*. Springer series in operations research and financial engineering. Springer, 2nd edition, 2006.
- R. Pamfil, N. Sriwattanaworachai, S. Desai, P. Pilgerstorfer, P. Beaumont, K. Georgatzis, and B. Aragam. DYNOTEARS: Structure learning from time-series data. In *International Conference on Artificial Intelligence and Statistics*, 2020.
- J. Pearl. *Probabilistic Reasoning in Intelligent Systems: Networks of Plausible Inference*. Morgan Kaufmann, 1988.
- J. Peters and P. Bühlmann. Identifiability of Gaussian structural equation models with equal error variances. *Biometrika*, 101(1):219–228, 2013.
- J. Peters, D. Janzing, and B. Schölkopf. *Elements of Causal Inference - Foundations and Learning Algorithms*. MIT Press, 2017.
- J. Ramsey, M. Glymour, R. Sanchez-Romero, and C. Glymour. A million variables and more: the fast greedy equivalence search algorithm for learning high-dimensional graphical causal models, with an application to functional magnetic resonance images. *International Journal of Data Science and Analytics*, 3(2):121–129, 2017.
- P. Ravikumar, M. J. Wainwright, G. Raskutti, and B. Yu. High-dimensional covariance estimation by minimizing ℓ_1 -penalized log-determinant divergence. *Electronic Journal of Statistics*, 5:935–980, 2011.
- A. Reisach, C. Seiler, and S. Weichwald. Beware of the simulated DAG! causal discovery benchmarks may be easy to game. In *Advances in Neural Information Processing Systems*, 2021.
- R. Scheines, P. Spirtes, C. Glymour, C. Meek, and T. Richardson. The TETRAD project: Constraint based aids to causal model specification. *Multivariate Behavioral Research*, 33:65–117, 1998.
- G. Schwarz. Estimating the dimension of a model. *The Annals of Statistics*, 6(2):461–464, 1978.
- S. Shimizu, P. O. Hoyer, A. Hyvärinen, and A. Kerminen. A linear non-Gaussian acyclic model for causal discovery. *Journal of Machine Learning Research*, 7(Oct):2003–2030, 2006.
- A. P. Singh and A. W. Moore. Finding optimal Bayesian networks by dynamic programming. Technical report, Carnegie Mellon University, 2005.
- P. Spirtes and C. Glymour. An algorithm for fast recovery of sparse causal graphs. *Social Science Computer Review*, 9:62–72, 1991.
- P. Spirtes, C. Glymour, and R. Scheines. *Causation, Prediction, and Search*. MIT press, 2nd edition, 2001.
- M. J. Wainwright. Sharp thresholds for high-dimensional and noisy sparsity recovery using ℓ_1 -constrained quadratic programming (Lasso). *IEEE Transactions on Information Theory*, 55(5):2183–2202, 2009.
- D. Wei, T. Gao, and Y. Yu. DAGs with no fears: A closer look at continuous optimization for learning Bayesian networks. In *Advances in Neural Information Processing Systems*, 2020.
- D. Xu, E. Gao, W. Huang, A. Song, and M. Gong. On the sparse DAG structure learning based on adaptive Lasso. *arXiv preprint arXiv:2209.02946*, 2022.
- M. Yang, F. Liu, Z. Chen, X. Shen, J. Hao, and J. Wang. CausalVAE: Disentangled representation learning via neural structural causal models. In *Proceedings of the IEEE Conference on Computer Vision and Pattern Recognition*, 2021a.

- S. Yang, K. Yu, F. Cao, L. Liu, H. Wang, and J. Li. Learning causal representations for robust domain adaptation. *IEEE Transactions on Knowledge and Data Engineering*, 2021b.
- Y. Yu, J. Chen, T. Gao, and M. Yu. DAG-GNN: DAG structure learning with graph neural networks. In *International Conference on Machine Learning*, 2019.
- Y. Yu, T. Gao, N. Yin, and Q. Ji. DAGs with no curl: An efficient DAG structure learning approach. In *International Conference on Machine Learning*, 2021.
- C. Yuan and B. Malone. Learning optimal Bayesian networks: A shortest path perspective. *Journal of Artificial Intelligence Research*, 48(1):23–65, 2013.
- Y. Zeng, S. Shimizu, R. Cai, F. Xie, M. Yamamoto, and Z. Hao. Causal discovery with multi-domain LiNGAM for latent factors. In *International Joint Conference on Artificial Intelligence*, 2021.
- C.-H. Zhang. Nearly unbiased variable selection under minimax concave penalty. *The Annals of Statistics*, 38(2):894–942, 2010.
- Z. Zhang, I. Ng, D. Gong, Y. Liu, E. M. Abbasnejad, M. Gong, K. Zhang, and J. Q. Shi. Truncated matrix power iteration for differentiable DAG learning. In *Advances in Neural Information Processing Systems (NeurIPS)*, 2022.
- X. Zheng. *Learning DAGs with Continuous Optimization*. PhD thesis, Carnegie Mellon University, 2020.
- X. Zheng, B. Aragam, P. Ravikumar, and E. P. Xing. DAGs with NO TEARS: Continuous optimization for structure learning. In *Advances in Neural Information Processing Systems*, 2018.
- X. Zheng, C. Dan, B. Aragam, P. Ravikumar, and E. P. Xing. Learning sparse nonparametric DAGs. In *International Conference on Artificial Intelligence and Statistics*, 2020.
- H. Zou. The adaptive Lasso and its oracle properties. *Journal of the American Statistical Association*, 101(476):1418–1429, 2006.

Appendices

A Discussion of Statements by Reisach et al. (2021)

We first list a few excerpts from Reisach et al. (2021):

- Abstract: “the remarkable performance of some continuous structure learning algorithms can be explained by high varsortability”.
- Section 1: “Our experiments demonstrate that varsortability dominates the optimization and helps achieve state-of-the-art performance provided the ground-truth data scale”.
- Section 3.4: “We explain how varsortability may dominate the performance of continuous structure learning algorithms”.
- Section 3.4: “For this reason we focus on the first optimization steps to explain a) why continuous structure learning algorithms that assume equal noise variance work remarkably well in the presence of high varsortability”.
- Section 4.3: “the evidence corroborates our claim that the remarkable performance on raw data and the overall behavior upon standardization of the continuous structure learning algorithms may be driven primarily by high varsortability”.

For clarity and ease of further analysis, we attempt to provide in Section 2.2 a partial formulation of the statements (on which this work focuses), separated into two different cases. In particular, we formulate Statements 1 and 2 by following the wordings from the fourth excerpt above because it has a relatively clear technical interpretation. Note that our analysis in Section 3 also applies if the statements are formulated based on some different excerpts. For instance, consider the following alternative formulations of the statements (that correspond to Statements 1 and 2, respectively) based on the second excerpt above.

Statement 3 (Equal Noise Variances Formulation). *Varsortability dominates the optimization of continuous structure learning approaches that assume equal noise variances, specifically NOTEARS-EV and GOLEM-EV, and helps them achieve state-of-the-art performance provided the ground-truth data scale.*

Statement 4 (Non-Equal Noise Variances Formulation). *Varsortability dominates the optimization of continuous structure learning approaches that assume non-equal noise variances, specifically GOLEM-NV, and helps them achieve state-of-the-art performance provided the ground-truth data scale.*

In particular, the examples in Section 3.1, i.e., Example 1 and Proposition 1, as well as the corresponding empirical studies, show that high varsortability does not help NOTEARS-EV and GOLEM-EV achieve a good performance, even when the ground-truth data scale is used. This is also the case for GOLEM-NV, as demonstrated in Section 3.2. These studies also suggest that varsortability may not dominate the optimization of these methods, at least in the settings considered.

B Proof of Proposition 1

It suffices to consider the distributions induced by the linear SEM with ground truth DAG specified in Figure 1a. Suppose that the weighted adjacency matrix B^* and noise covariance matrix Ω^* are defined by

$$B^* = \begin{bmatrix} 0 & a & b \\ 0 & 0 & c \\ 0 & 0 & 0 \end{bmatrix}, \quad \Omega^* = \begin{bmatrix} \sigma_1^2 & 0 & 0 \\ 0 & \sigma_2^2 & 0 \\ 0 & 0 & \sigma_3^2 \end{bmatrix},$$

where $a, b, c \neq 0$ and $\sigma_1, \sigma_2, \sigma_3 > 0$. In the large sample limit, the covariance matrix of X is

$$\begin{aligned}\Sigma^* &= (I - B^*)^{-T} \Omega^* (I - B^*)^{-1} \\ &= \begin{bmatrix} \sigma_1^2 & a\sigma_1^2 & \sigma_1^2(ac+b) \\ a\sigma_1^2 & a^2\sigma_1^2 + \sigma_2^2 & a\sigma_1^2(ac+b) + c\sigma_2^2 \\ \sigma_1^2(ac+b) & a\sigma_1^2(ac+b) + c\sigma_2^2 & c^2\sigma_2^2 + \sigma_1^2(ac+b)^2 + \sigma_3^2 \end{bmatrix},\end{aligned}$$

and the varsortability equals one if

$$a^2\sigma_1^2 - \sigma_1^2 + \sigma_2^2 > 0, \quad (2)$$

$$-a^2\sigma_1^2 + c^2\sigma_2^2 + \sigma_1^2(ac+b)^2 - \sigma_2^2 + \sigma_3^2 > 0. \quad (3)$$

With a slight abuse of notation, the least squares loss w.r.t. any weighted matrix B is

$$\ell(B; \Sigma^*) = \frac{1}{2} \text{tr}((I - B)^T \Sigma^* (I - B)).$$

Consider another weighted adjacency matrix

$$\tilde{B} = \begin{bmatrix} 0 & 0 & 0 \\ \tilde{a} & 0 & \tilde{c} \\ \tilde{b} & 0 & 0 \end{bmatrix},$$

which corresponds to the DAG in Figure 1b. Solving

$$\frac{\partial \ell(\tilde{B}; \Sigma^*)}{\partial \tilde{a}} = \frac{\partial \ell(\tilde{B}; \Sigma^*)}{\partial \tilde{b}} = \frac{\partial \ell(\tilde{B}; \Sigma^*)}{\partial \tilde{c}} = 0$$

leads to the solution

$$\hat{B} = \begin{bmatrix} 0 & 0 & 0 \\ \frac{\sigma_1^2(a\sigma_3^2 - bc\sigma_2^2)}{a^2\sigma_1^2\sigma_3^2 + b^2\sigma_1^2\sigma_2^2 + \sigma_2^2\sigma_3^2} & 0 & \frac{a^2c\sigma_1^2 + ab\sigma_1^2 + c\sigma_2^2}{a^2\sigma_1^2 + \sigma_2^2} \\ \frac{b\sigma_1^2\sigma_2^2}{a^2\sigma_1^2\sigma_3^2 + b^2\sigma_1^2\sigma_2^2 + \sigma_2^2\sigma_3^2} & 0 & 0 \end{bmatrix},$$

which implies that $\ell(\hat{B}; \Sigma^*)$ is minimized at \hat{B} . If $\ell(\hat{B}; \Sigma^*) < \ell(B^*; \Sigma^*)$, then the DAG in Figure 1b leads to a lower least squares score than that of the true DAG. A simple calculation of $\ell(\hat{B}; \Sigma^*) < \ell(B^*; \Sigma^*)$ yields the inequality

$$-a^2\sigma_1^2 - \frac{\sigma_1^2\sigma_2^2\sigma_3^2}{a^2\sigma_1^2\sigma_3^2 + b^2\sigma_1^2\sigma_2^2 + \sigma_2^2\sigma_3^2} + \sigma_1^2 + \sigma_3^2 - \frac{a^2\sigma_1^2\sigma_3^2 + b^2\sigma_1^2\sigma_2^2 + \sigma_2^2\sigma_3^2}{a^2\sigma_1^2 + \sigma_2^2} > 0. \quad (4)$$

The following lemma concludes the proof of the proposition.

Lemma 1. *The set of solutions to inequalities (2), (3), and (4) has a nonzero Lebesgue measure.*

Proof of Lemma 1. We provide a constructive proof by constructing a subset of the solutions with a nonzero Lebesgue measure to the inequalities (2), (3), and (4).

By inequality (2), we have

$$a^2 > 1 - \frac{\sigma_2^2}{\sigma_1^2}. \quad (5)$$

By rearranging the terms in inequality (3), we have

$$(a^2\sigma_1^2 + \sigma_2^2)c^2 + (2ab\sigma_1^2)c + (b^2\sigma_1^2 - a^2\sigma_1^2 - \sigma_2^2 + \sigma_3^2) > 0.$$

The LHS of the above inequality can be viewed as a quadratic function with variable c , which we denote by $f(c)$. For any values of $a, b, \sigma_1, \sigma_2, \sigma_3$, since the coefficient of quadratic term c^2 is positive, i.e., $a^2\sigma_1^2 + \sigma_2^2 > 0$,

function $f(c)$ corresponds to a parabola that opens upwards. Therefore, for any values of $a, b, \sigma_1, \sigma_2, \sigma_3$, the set of solutions for c that lead to $f(c) > 0$ (and thus inequality (3)) has a nonzero measure on \mathbb{R} .

We now turn to inequality (4). Substituting $k = a^2\sigma_1^2\sigma_3^2 + b^2\sigma_1^2\sigma_2^2 + \sigma_2^2\sigma_3^2$ into inequality (4) and rearranging, we obtain

$$-k^2 + (a^2\sigma_1^2 + \sigma_2^2)(\sigma_1^2 - a^2\sigma_1^2 + \sigma_3^2)k - (a^2\sigma_1^2 + \sigma_2^2)\sigma_1^2\sigma_2^2\sigma_3^2 > 0. \quad (6)$$

The LHS of the above inequality can be viewed as a quadratic function with variable k , which we denote as $g(k)$. For any values of $a, \sigma_1, \sigma_2, \sigma_3$, since the coefficient of quadratic term k^2 is negative, function $g(k)$ corresponds to a parabola that opens downwards. For any values of $a, \sigma_1, \sigma_2, \sigma_3$, our goal is such that the set of solutions for k which satisfy inequality (6) and $k > a^2\sigma_1^2\sigma_3^2 + \sigma_2^2\sigma_3^2$ has a nonzero measure on \mathbb{R} , so that the set of solutions for b has a nonzero measure on \mathbb{R} . To achieve that, it suffices to enforce the following: (i) the x-coordinate of the vertex of function $g(k)$ is larger than $a^2\sigma_1^2\sigma_3^2 + \sigma_2^2\sigma_3^2$, i.e.,

$$-\frac{(a^2\sigma_1^2 + \sigma_2^2)(\sigma_1^2 - a^2\sigma_1^2 + \sigma_3^2)}{2(-1)} > a^2\sigma_1^2\sigma_3^2 + \sigma_2^2\sigma_3^2 \iff a^2 < 1 - \frac{\sigma_3^2}{\sigma_1^2}, \quad (7)$$

and (ii) the discriminant of function $g(k)$ is positive, i.e.,

$$(a^2\sigma_1^2 + \sigma_2^2)^2(\sigma_1^2 - a^2\sigma_1^2 + \sigma_3^2)^2 - 4(-1)(a^2\sigma_1^2 + \sigma_2^2)(-a^2\sigma_1^2\sigma_3^2 - \sigma_2^2\sigma_3^2) > 0,$$

or equivalently,

$$(a^2\sigma_1^2 + \sigma_2^2)(\sigma_1^2 - a^2\sigma_1^2 + \sigma_3^2)^2 > 4\sigma_1^2\sigma_2^2\sigma_3^2.$$

With $a^2\sigma_1^2 + \sigma_2^2 > \sigma_1^2$ from inequality (2), in order for the above inequality to hold, it suffices to enforce

$$(\sigma_1^2 - a^2\sigma_1^2 + \sigma_3^2)^2 > 4\sigma_2^2\sigma_3^2, \quad (8)$$

which, with simple calculation, indicates the solution

$$a^2 < 1 + \frac{(\sigma_3 - 2\sigma_2)\sigma_3}{\sigma_1^2} \quad \text{or} \quad a^2 > 1 + \frac{(\sigma_3 + 2\sigma_2)\sigma_3}{\sigma_1^2}.$$

Here, we pick

$$a^2 < 1 + \frac{(\sigma_3 - 2\sigma_2)\sigma_3}{\sigma_1^2}.$$

Combining the above inequality with inequalities (5) and (7), we have

$$\max\left(0, 1 - \frac{\sigma_2^2}{\sigma_1^2}\right) < a^2 < \min\left(1 - \frac{\sigma_3^2}{\sigma_2^2}, 1 + \frac{(\sigma_3 - 2\sigma_2)\sigma_3}{\sigma_1^2}\right). \quad (9)$$

For a to have a set of solutions with nonzero measure in the inequality above, we need

$$\max\left(0, 1 - \frac{\sigma_2^2}{\sigma_1^2}\right) < \min\left(1 - \frac{\sigma_3^2}{\sigma_2^2}, 1 + \frac{(\sigma_3 - 2\sigma_2)\sigma_3}{\sigma_1^2}\right),$$

which, by some algebraic manipulations, implies

$$0 < \sigma_3 < \sigma_1 \quad \text{and} \quad \sqrt{\sigma_1\sigma_3} < \sigma_2 < \frac{\sigma_1^2 + \sigma_3^2}{2\sigma_3}. \quad (10)$$

Therefore, if $a, \sigma_1, \sigma_2, \sigma_3$ satisfy inequalities (10) and (9), then they also satisfy inequalities (8) and (7). For these values of $a, \sigma_1, \sigma_2, \sigma_3$, this implies that the set of solutions for k that satisfy inequality (6) and $k > a^2\sigma_1^2\sigma_3^2 + \sigma_2^2\sigma_3^2$ has a nonzero measure on \mathbb{R} , indicating that the set of solutions for b has a nonzero measure on \mathbb{R} , because we have

$$b^2 = \frac{k - a^2\sigma_1^2\sigma_3^2 - \sigma_2^2\sigma_3^2}{\sigma_1^2\sigma_2^2}.$$

Combining all three cases, the set of solutions we construct here to inequalities (2), (3), and (4) has a nonzero Lebesgue measure, which clearly is a subset of the complete set of solutions. Thus, the complete set of solutions to inequalities (2), (3), and (4) has a nonzero Lebesgue measure. \square

C Analysis of Non-Equal Noise Variances Formulation

C.1 Alternative Form of Likelihood Function

In the derivation of GOLEM-NV (Ng et al., 2020, Appendix C.1), the resulting optimization problem in Eq. (1) involves only the matrix B because it profiles out the parameter Ω that corresponds to the noise variances. Here, we consider the form of likelihood function without profiling out such parameter. Specifically, we consider the optimization problem

$$\min_{\substack{B \in \mathbb{R}^{d \times d} \\ \sigma_1, \dots, \sigma_d > 0}} \mathcal{L}_{\text{NV}}(B, \sigma_1, \dots, \sigma_d; \mathbf{X}) - \log |\det(I - B)| + \lambda_1 \|B\|_1 + \lambda_2 h(B), \quad (11)$$

where

$$\mathcal{L}_{\text{NV}}(B, \sigma_1, \dots, \sigma_d; \mathbf{X}) = \frac{1}{2} \sum_{i=1}^d \left(\log \sigma_i^2 + \frac{\|\mathbf{X}_{\cdot, i} - \mathbf{X}B_{\cdot, i}\|_2^2}{n\sigma_i^2} \right).$$

We consider the same setting in Section 4.1, and report the empirical results in Figure 12. One observes that both forms of likelihood functions with and without profiling out the noise variances lead to a poor performance (when initialized with zero matrix) even when the sample size is large. For instance, with 10^6 samples, the SHDs of GOLEM with and without profiling are 121.4 ± 3.0 and 79.0 ± 3.3 , respectively, while PC and FGES have much lower SHDs at 5.2 ± 0.6 and 5.0 ± 0.8 , respectively. This suggests that both forms of likelihood functions may be susceptible to suboptimal local solutions possibly owing to nonconvexity.

Similar to the initialization strategy described in Section 3.2, we also considered using the the solution of FGES to initialize the optimization problem (11), by computing the initial solution of weighted matrix B and noise variances $\sigma_1, \dots, \sigma_d$. A similar observation in Figure 4 is obtained, i.e., such an initialization strategy improves the performance of structure learning, which indicates that the alternative formulation of GOLEM-NV in Eq. (11) also depends largely on the initial solution.

It is worth noting that we also conducted the same experiments above with NOTEARS by replacing its least squares objective with $\mathcal{L}_{\text{NV}}(B, \sigma_1, \dots, \sigma_d; \mathbf{X})$ to handle the non-equal noise variances case, and have the same observations (the empirical results are omitted here for brevity).

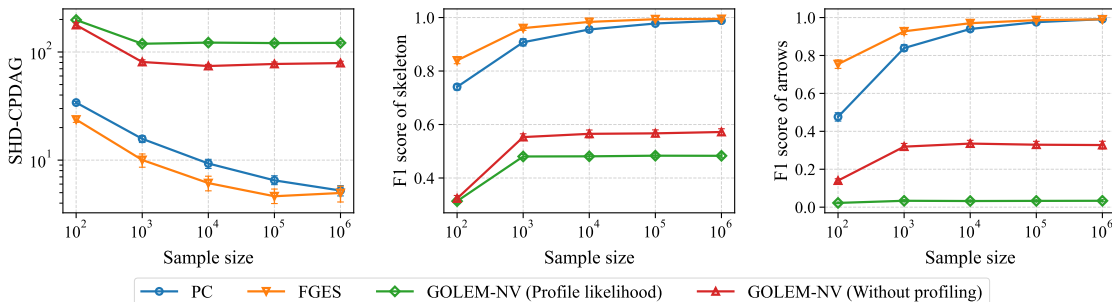


Figure 12: Empirical results of different forms of likelihood function under different sample sizes. The number of variables is 50. Error bars represent the standard errors computed over 30 random repetitions.

C.2 Nonconvexity

We investigate the connection between the score function of GOLEM-NV and the quality of the estimated structure. Specifically, we consider GOLEM-NV initialized by zero matrix as well as by solutions of GOLEM-EV and FGES. We also include the comparison with zero matrix and random DAG. For these methods, we compute the SHD of the estimated CPDAGs, and the score of GOLEM-NV (before thresholding) given in problem (1). We consider 50-node ER1 graphs with a noise ratio of 16.

The results are reported in Figure 13. One observes that GOLEM-NV initialized by GOLEM-EV and by FGES achieves a low score that is close to the score of the true DAG. At the same time, they also have a low SHD, indicating that their estimated structures are close to the true CPDAGs. However, this is not the case for GOLEM-NV initialized by zero matrix. Specifically, it also achieves a score that is very close to that of the true DAG, but its SHD is 127.43 ± 2.98 . This appears to suggest that (1) a lower score does not necessarily lead to a low SHD-CPDAG, and (2) the nonconvex landscape of GOLEM-NV may contain suboptimal solutions whose scores are very close to the score of the global minimizer, but their corresponding structures may be very far from the true CPDAG. Thus, this demonstrates that nonconvexity may be a severe concern, at least in this setting considered.

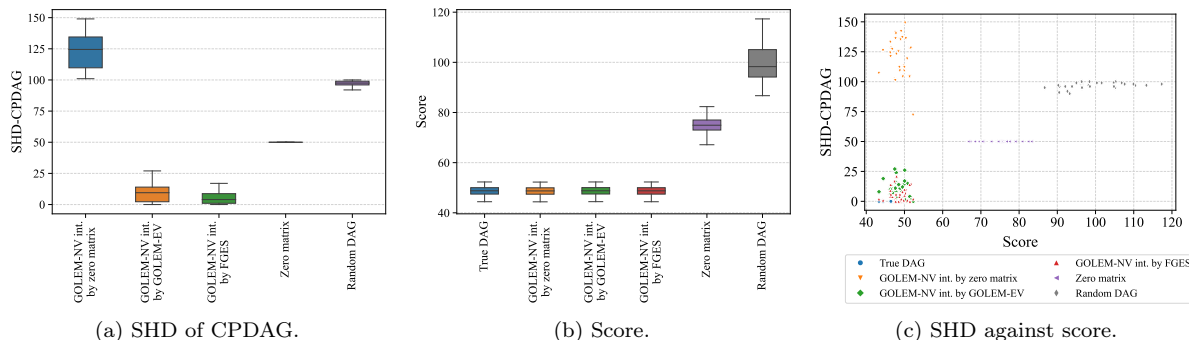


Figure 13: Visualization of SHD and score for different methods over 30 random repetitions.. Lower is better for both SHD and score.

D Supplementary Experiment Details

In this section we provide supplementary experiment details for Sections 3.1, 3.2, 4.1, 4.2, 4.3, 5.1, and 5.2.

D.1 Implementation Details and Hyperparameters

For the structure learning methods considered, we use the default hyperparameters and official implementations from the authors, unless otherwise stated. As suggested in Section 5.1, using a relatively large threshold of 0.3 as in existing works may be harmful and remove many true edges, especially when the edge weights in the true weighted adjacency matrix are small. In this work, we consider a smaller threshold of 0.1. Furthermore, for NOTEARS-NV, DPDAG-NV, DAGMA-NV, and NOCURL-NV, we use the same hyperparameter as GOLEM-NV for sparsity penalty, i.e., $\lambda = 0.002$.

We provide further details for specific methods as follows:

- GOLEM: We use L-BFGS (Byrd et al., 1995) to solve the unconstrained optimization problem as it runs faster than Adam (Kingma and Ba, 2014) and leads to a similar performance.
- NOTEARS: We use the quadratic penalty method instead of augmented Lagrangian method to solve the constrained optimization problem, since Ng et al. (2022b) showed that their performance is nearly identical, and that the former converges in a fewer number of iterations.
- A*: We adapt an implementation from the `causal-learn` package available at the GitHub repository <https://github.com/cmu-phil/causal-learn>, and modify the BIC score (Schwarz, 1978) to least squares score (Loh and Bühlmann, 2014). We set the coefficient of ℓ_0 penalty to 0.01.
- GDS: We use our own implementation in Python. A noticeable difference with the algorithm described by Peters and Bühlmann (2013) is that we use the least squares score (Loh and Bühlmann, 2014)

instead of likelihood score, both of which assume equal noise variances. We set the coefficient of ℓ_0 penalty to 0.01.

- PC, FGES: We use the implementation from the `py-causal` package available at the GitHub repository <https://github.com/bd2kccd/py-causal>, which is a Python wrapper of the TETRAD project (Scheines et al., 1998). We adopt the Fisher Z test and BIC score (Schwarz, 1978) for PC and FGES, respectively.

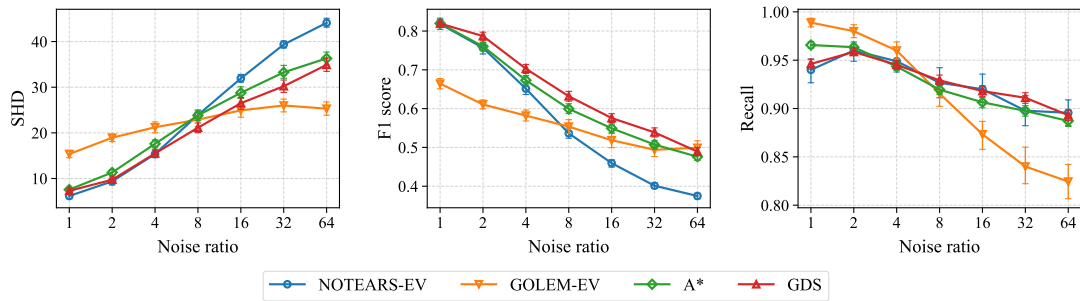
D.2 Discussion of Search Strategies

As discussed in Section 2.1, NOTEARS (Zheng et al., 2018) solves a constrained optimization problem with a hard DAG constraint by leveraging augmented Lagrangian or quadratic penalty method (Bertsekas, 1982, 1999), while GOLEM (Ng et al., 2020) solves an unconstrained optimization with a soft DAG constraint. These essentially represent different strategies to search for a DAG. Similar to NOTEARS, DAGMA (Bello et al., 2022) solve a constrained optimization problem, but adopts a procedure similar to the barrier method (Nocedal and Wright, 2006) with a log-determinant DAG constraint. Instead of enforcing DAGs via a constrained optimization problem like NOTEARS and DAGMA, another line of approaches directly search in the space of DAGs. Specifically, NOCURL (Yu et al., 2021) developed an algebraic representation of DAGs based on graph Hodge theory (Jiang et al., 2011; Bang-Jensen and Gutin, 2009) that directly outputs weighted adjacency matrix of a DAG, while DPDAG (Charpentier et al., 2022) developed a differentiable DAG sampling procedure that (1) samples a linear ordering of the variables using Gumbel-Sinkhorn (Mena et al., 2018) or Gumbel-Top-k (Kool et al., 2019) reparametrizations, and (2) samples a weighted adjacency matrix consistent with the ordering. Note that DPDAG was combined with variational inference and MLPs, which leads to the VI-DP-DAG approach for the nonlinear case, and here we adapt it to learn linear DAGs (without the parts of variational inference and MLPs). These several approaches represent different strategies to traverse the search space for estimating a DAG with continuous optimization.

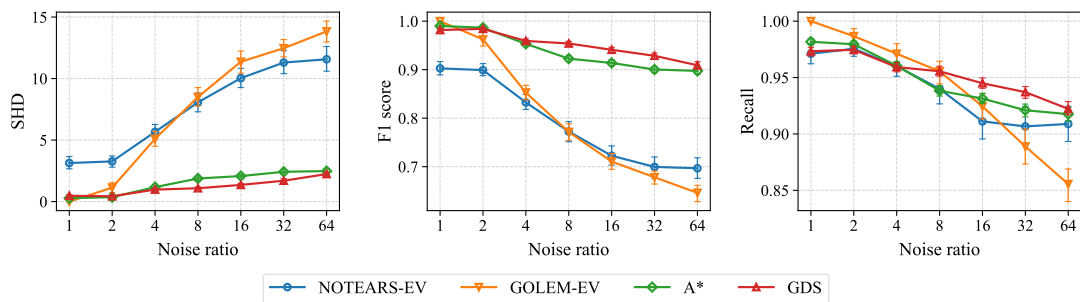
E Supplementary Experiment Results

In this section, we provide supplementary experiment results for Sections 3.1, 3.2, 4.1, 4.2, 4.3, 5.1, and 5.2.

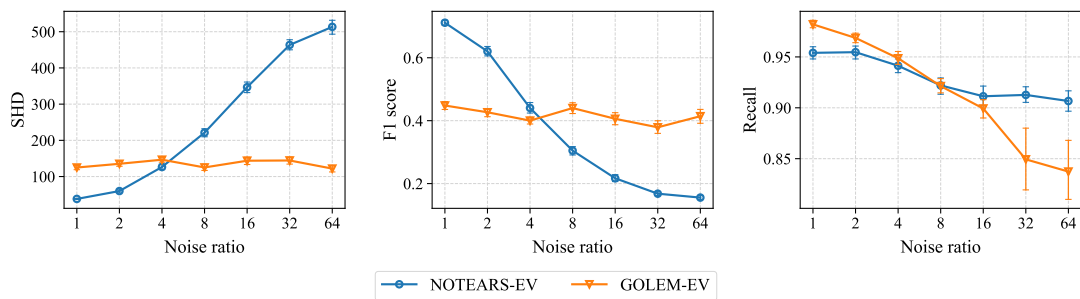
E.1 Varsortability & Data Standarziation: Equal Noise Variances Formulation



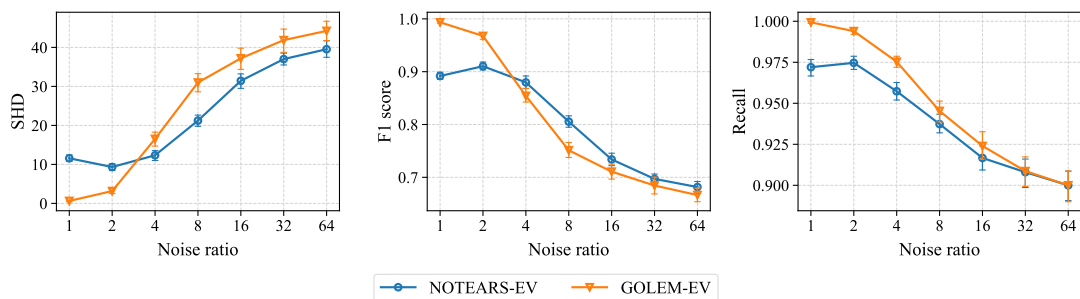
(a) 15 variables with 100 samples.



(b) 15 variables with 10^6 samples.



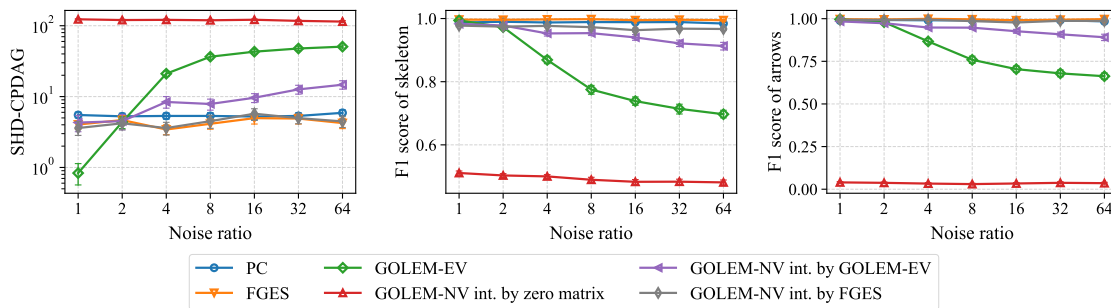
(c) 50 variables with 100 samples.



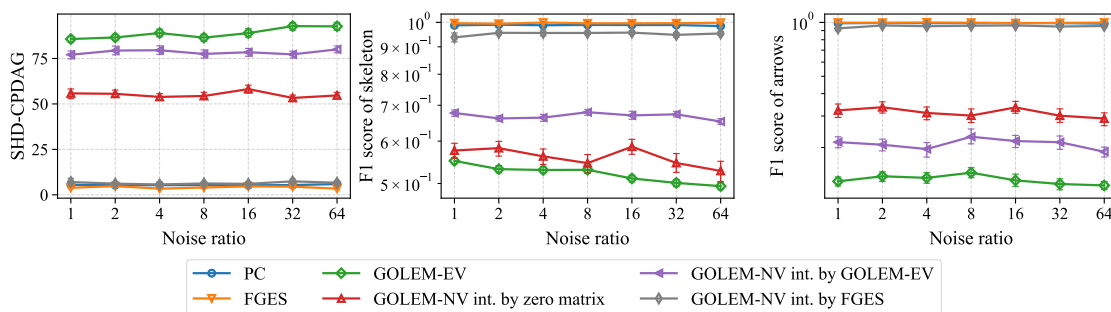
(d) 15 variables with 10^6 samples.

Figure 14: Empirical results of structure learning methods assuming equal noise variances under different noise ratios. Error bars represent the standard errors computed over 30 random repetitions.

E.2 Varsortability & Data Standarziation: Non-Equal Noise Variances Formulation



(a) Without data standardization.



(b) With data standardization.

Figure 15: Empirical results of structure learning methods under different noise ratios. The number of variables is 50 and the sample size is 10^6 . Error bars represent the standard errors computed over 30 random repetitions.

E.3 Search Strategies

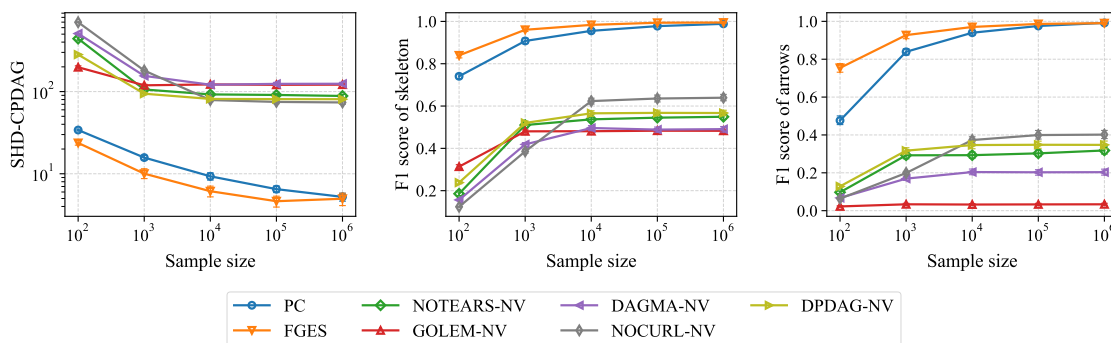
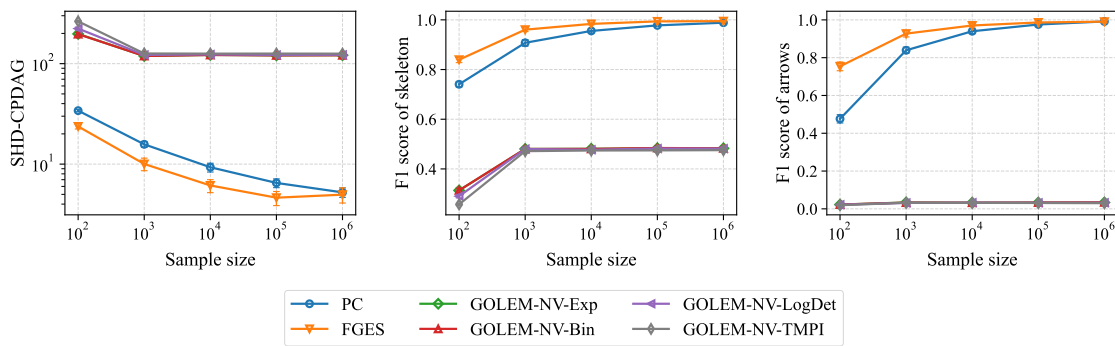
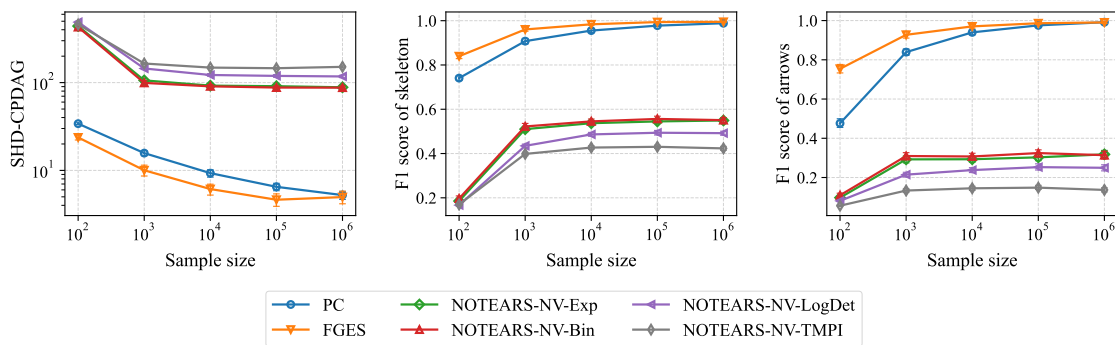


Figure 16: Empirical results of different search strategies under different sample sizes. The number of variables is 50. Error bars represent the standard errors computed over 30 random repetitions.

E.4 DAG Constraints



(a) GOLEM-NV with different DAG constraints.



(b) NOTEARS-NV with different DAG constraints.

Figure 17: Empirical results of different DAG constraints under different sample sizes. The number of variables is 50. Error bars represent the standard errors computed over 30 random repetitions.

E.5 Other Cases

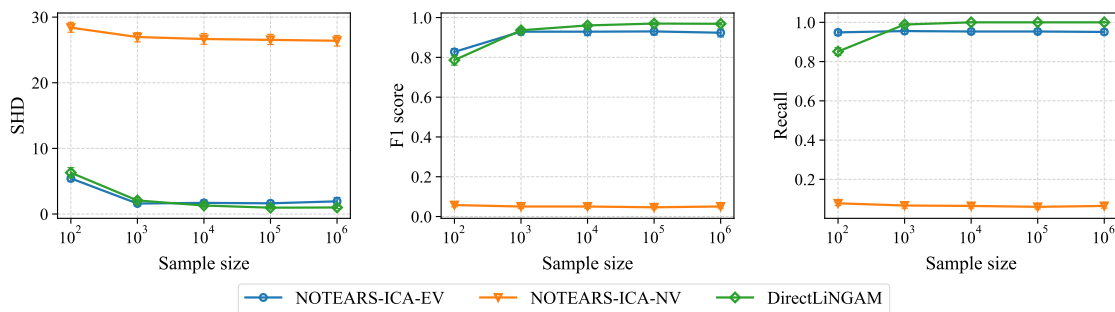


Figure 18: Empirical results of NOTEARS-ICA under different sample sizes. The number of variables is 15. Error bars represent the standard errors computed over 30 random repetitions.

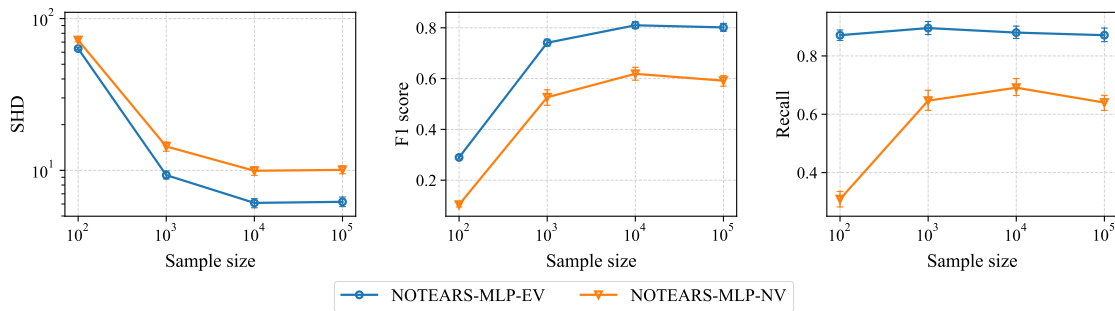
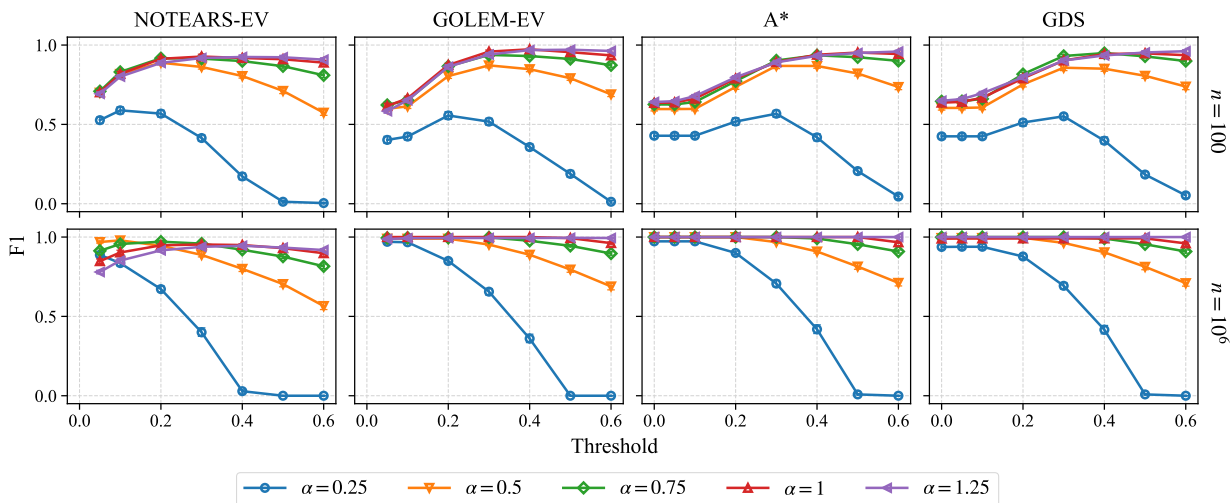
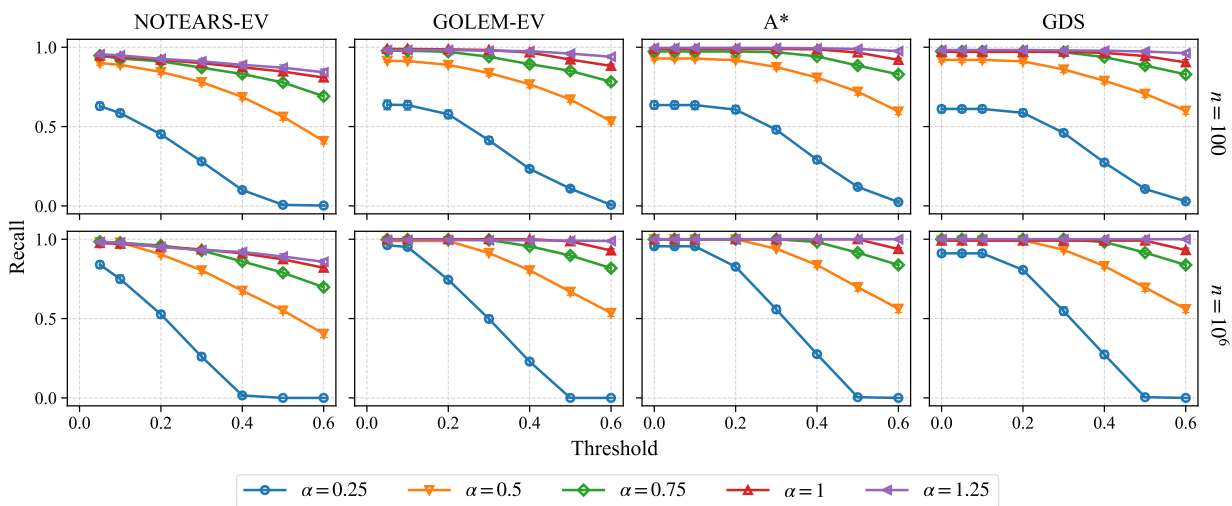


Figure 19: Empirical results of NOTEARS-MLP under different sample sizes. The number of variables is 15. Error bars represent the standard errors computed over 30 random repetitions.

E.6 Thresholding



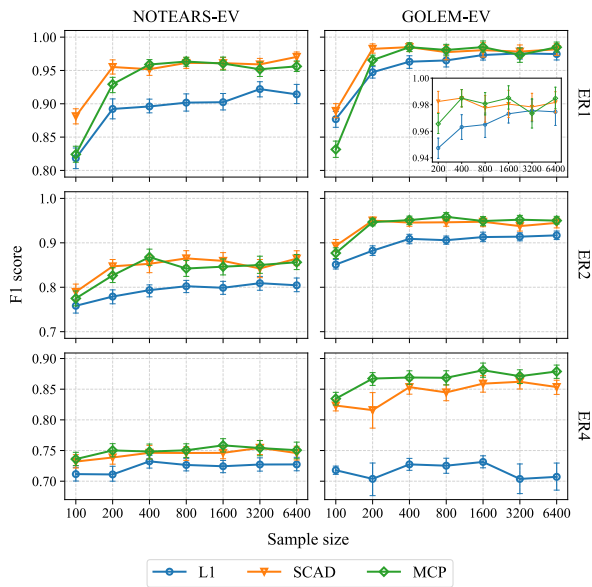
(a) F1 score.



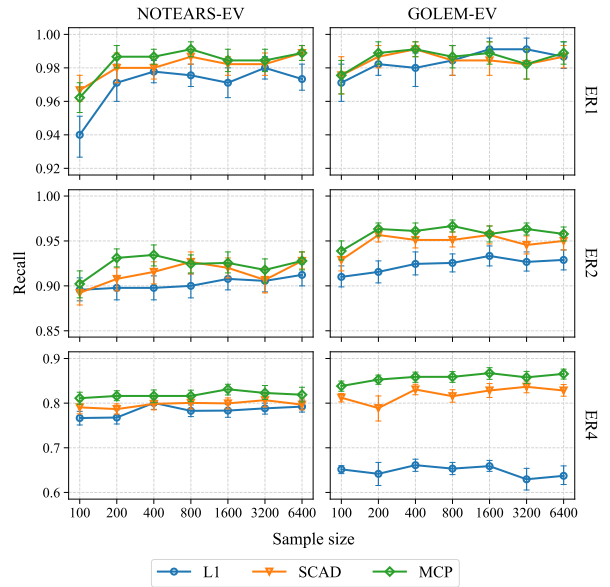
(b) Recall.

Figure 20: Empirical results of different thresholds under different weight scales. The number of variables is 15. Error bars represent the standard errors computed over 30 random repetitions.

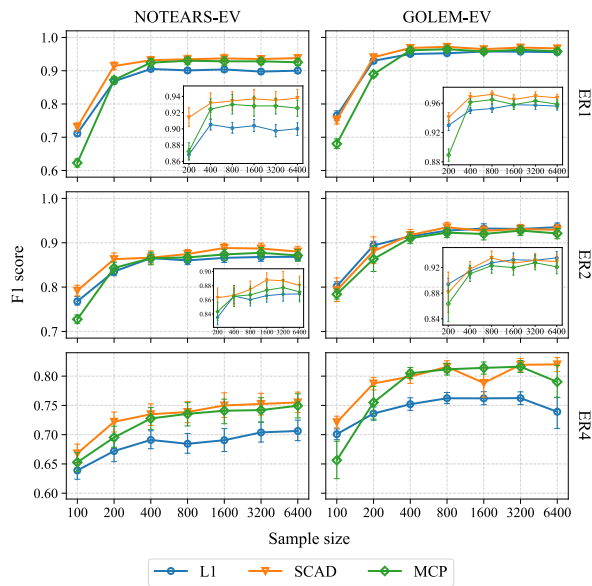
E.7 Sparsity Penalty



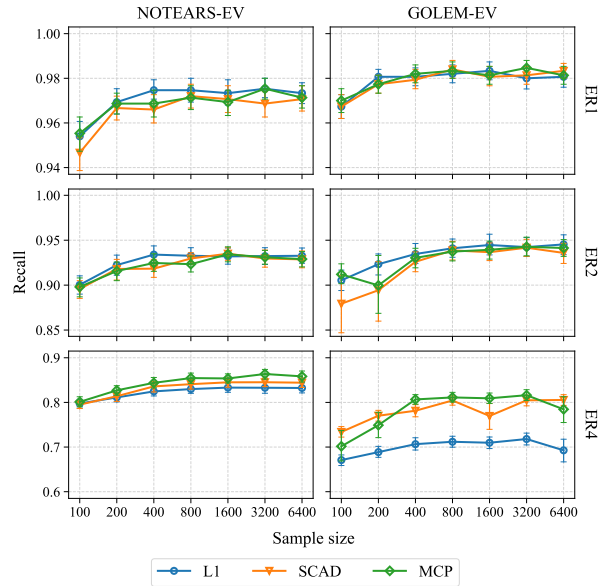
(a) F1 score for 15 variables case.



(b) Recall for 15 variables case.



(c) F1 score for 50 variables case.



(d) Recall for 50 variables case.

Figure 21: Empirical results of different sparsity penalties under different sample sizes. Error bars represent the standard errors computed over 30 random repetitions.